

Stability in human interaction networks: primitive typology of vertex, prominence of measures and activity statistics

Renato Fabbri,^{1, a)} Vilson V. da Silva Jr.,^{b)} Ricardo Fabbri,^{c)} Deborah C. Antunes,^{d)} and Marília M. Pisani^{e)}
São Carlos Institute of Physics, University of São Paulo (IFSC/USP)

(Dated: 1 March 2015)

This article reports interaction networks stability by means of three quantitative criteria: activity distribution in time and among participants; a sound classification of vertices in peripheral, intermediary and hub sectors; the combination of basic measures into principal components with greater variance. We analyzed the temporal activity and topology evolution of networks in four email lists by considering window sizes from 50 to 10,000 messages, which were made to slide to generate snapshots of the network along a timeline. Activity in terms of seconds, minutes, days and months was remarkably similar for all the networks. Participant activity follows concentrations expected in scale-free networks. We compare these networks to Erdős-Rényi networks in order to assign members to three distinct sectors, namely hubs, intermediary and periphery. The fractions of members in these sectors were essentially the same for all networks and, most importantly, stable over time. If strength is used as the criterion for classification, for instance, ca. 5% of the vertices are hubs, 15-20% are intermediary and the remainder compose periphery. The metrics most representative for data dispersion were found to be centrality-related (degree, strength and betweenness), followed by symmetry-related, and then clustering coefficient. Degree, strength and clustering cope with different symmetry measures to bear secondary components. Again, the importance of these metrics to network topology dispersion was practically the same for all email lists examined, and stable over time. The research also resulted on a sketch of a physics-based typology of agents, with proper social and psychological speculations. Because the network properties reported did not depend on the email list and were stable over time, and because observed structure is in accordance with expectations driven from literature for human interaction networks, we believe that the properties observed holds for general human interaction networks, and the approach can be applied to other types of networks. Current unfoldings include governance and accountability proposals and implementations, anthropological physics experiments and the report of quantitative differences of textual production as connectivity of agents changes.

PACS numbers: 89.75.Fb, 05.65.+b, 89.65.-s

Keywords: complex networks, social network analysis, pattern recognition, statistics, anthropological physics

‘The reason for the persistent plausibility of the typological approach, however, is not a static biological one, but just the opposite: dynamic and social. The fact that human society has been up to now divided into classes affects more than the external relations of men. The marks of social repression are left within the individual soul.’

- Adorno et al, 1969, p. 747

I. INTRODUCTION

The present work is aimed at finding common characteristics among (email) interaction networks. This includes observations along time, which imply network evolution, a field that has received dedicated attention from the research community for more than a decade^{1,2}.

While significant measures will depend on the model and system characteristics^{3,4}, this work considers only directed, weighted and human interaction networks. Undirected and unweighted representation of such networks is also found in the literature and can be obtained by simplification⁵.

Text mining and typologies of online participants benefit from the results here presented^{6,7}. Although all networks considered originated from email lists, coherence with literature suggests that results hold for a more general class of interaction networks, such as observed in online platforms (e.g. LinkedIn, Facebook, Twitter).

A. Related work

This work approaches network stability through temporal evolution observation. The evolution is represented

^{a)} <http://ifsc.usp.br/~fabbri/>; Electronic mail: fabbri@usp.br

^{b)} <http://automata.cc/>; Electronic mail: vilson@void.cc; Also at IFSC-USP

^{c)} <http://www.lems.brown.edu/~rfabbri/>; Electronic mail: rfabbri@iprj.uerj.br; Instituto Politécnico, Universidade Estadual do Rio de Janeiro (IPRJ)

^{d)} <http://lattes.cnpq.br/1065956470701739>; Electronic mail: deborahantunes@gmail.com; Curso de Psicologia, Universidade Federal do Ceará (UFC)

^{e)} <http://lattes.cnpq.br/6738980149860322>; Electronic mail: marilia.m.pisani@gmail.com; Centro de Cincias Naturais e Humanas, Universidade Federal do ABC (CCNH/UFABC)

by a timeline of activity snapshots with a constant number of contiguous messages. These snapshots yield a succession of networks. This approach, although coherent and intuitive, seems not to be explored to date⁸.

Works on network evolution often consider solely network growth, in which there is a monotonic increase in the number of events considered¹. Exceptions are reported in this section, specially those more closely related to the present article.

The evolution of human interaction networks was addressed with a community focus, where the direction of edges was not taken into account¹. In another article, two topologically different networks emerged from human interaction networks, depending on the frequency of interactions, which could either be a generalized power law or an exponential connectivity distribution⁹. In email list networks, scale-free properties were verified¹⁰, and different linguistic traces were related to weak and strong ties⁵.

Unreciprocated edges often exceed 50% in the networks analyzed, which matches empirical evidence². No correlation of topological characteristics and geographical position was found⁴³, therefore geographical incidences was discarded in the present article. On the other hand, gender related behavior in mobile phone datasets has been reported⁴⁷ and was not considered in this article as the email messages and addresses have no gender related metadata¹². Controllability of these networks is also an uncovered issue. These has unintuitive properties and might bring into forefront crucial properties^{44–46}, which might be the subject of subsequent research.

The seminal Nature Letter by Palla, Barabási and Vicsek¹ has strong confluence with this work, suggesting that the smaller size of MET community is responsible for the stronger hubs observed.

These results are corroborated by phenomena reported in this paper, which is an indicative that the stability reported herein is common to general human interaction networks.

B. Paired article to analyse textual production

Significant differences in the textual production of each connective sector of the network (periphery, intermediary, hubs) is reported in an article by the same research group⁶. Most importantly, linguistic differences are more prominent between the sectors of a same network than between the same sector in different lists.

C. The Versinus visualization method for evolving complex networks

To visualize network evolution, the Versinus method was developed. The method is simple and consists in the placement of each vertex along a sinusoid and a line. In the resulting fixed layout, the time evolution takes

place. Even so, fellow researchers repeatedly asked for an article describing Versinus, and therefore it was written in 2013¹¹.

D. Typology of online agents

A core purpose of the present article, dedicated to stability in interaction networks, and the article about textual production⁶ is to derive a sound typology of online agents, with quantitative criteria driven from physics (to the extent possible). This is a work under construction, with preliminary elaborations in Section IV D, but should be extensively published in near future.

II. DATA DESCRIPTION

A. Email lists and messages

Email list messages were obtained from the GMANE email archive¹², which consists of more than 20,000 email lists and more than 130,000,000 messages¹³. These lists cover a variety of topics, mostly technology-related. The archive can be described as a corpus with metadata of its messages, including sent time, place, sender name, and sender email address. The GMANE usage in scientific research is reported in studies of isolated lists and of lexical innovations^{5,10}. The computer scripts for gathering and processing GMANE email messages are given in Appendix B.

Four email lists were selected for their diversity, making it easier to infer general properties.

- Linux Audio Users list¹⁴. Dominated by participants with hybrid artistic and technological interests. Participants are from different countries, and English is the language used the most. Abbreviated as LAU from now on.
- Linux Audio Developers list¹⁵. Participants are from different countries, and English is the language used the most. A more technical and less active version of LAU. Abbreviated LAD from now on.
- Development list for the standard C++ library¹⁶. Dominated by specialized computer programmers. Participants are from different countries, and English is the language used the most. Abbreviated as CPP from now on.
- List of the MetaReciclagem project¹⁷. Dominated by Brazilian activists and digital culture interests. Participants are mostly Brazilians, and Portuguese is the most used language, although Spanish and English are also incident. Abbreviated MET from now on.

TABLE I. Columns $date_1$ and $date_M$ have dates of first and last messages from the 20,000 messages considered in each email list. N is the number of participants (number of different email addresses). Γ is the number of threads (count of messages without antecedent). \bar{M} is the number of messages missing in the 20,000 collection, $100 - \frac{23}{20000} = 0.115$ percent in the worst case. MET notably has the fewer participants and the larger number of threads. This relation holds for each of the lists considered here and a derived article (see Section IB): as the number of participants increases, the number of threads decreases.

list	$date_1$	$date_M$	N	Γ	\bar{M}
LAU	Jun/29/2003	Jul/23/2005	1183	3373	5
LAD	Jun/30/2003	Oct/07/2009	1268	3113	4
MET	Ago/01/2005	Mar/07/2008	492	4607	23
CPP	Mar/13/2002	Aug/25/2009	1052	4506	7

The first 20,000 messages of each list were considered, with total timespan, authors, threads and missing messages, as indicated in Table I.

III. CHARACTERIZATION METHODS

The email lists and the networks generated from them were characterized by: 1) statistics of activity along time, with a detailed analysis for time durations from seconds to years; 2) sectioning of the networks in hubs, intermediary and peripheral vertices; 3) prominence of topological measures, including their time dependence; 4) iterative visualization and data mining of networks; 5) typological elaborations of networks and participants. Each of these procedures are described below with supporting structures.

Distribution of activity among participants are in Table V and indirectly through almost all results of this article, as degree and strength are highly correlated to activity.

A. Time activity statistics

Messages were counted along time with respect to seconds, minutes, hours, days of the week, days of the month, and months of the year. These are exhibited as Tables VI-IX in Appendix C2. Results are outlined in Section IV A.

B. Interaction network

Regarding literature^{10,18,19}, interaction networks can be modeled both weighted or unweighted, both directed or undirected. Networks in this article are directed and weighted, the more informative of trivial possibilities, i.e. we did not observe directed unweighted, undirected weighted, and undirected unweighted representations of the interaction network. The networks were obtained as

follows: a direct response from participant B to a message from participant A yields an edge from A to B, as information went from A to B. The reasoning is: if B wrote a response to a message from A, he/she read what A wrote and formulated a response, so B assimilated information from A, thus $A \rightarrow B$. Inverting edge direction yields the status network: B read the message and considered what A wrote worth responding, giving status to A, thus $B \rightarrow A$. This article uses the information network as described above and depicted in Figure 1. Edges in both directions are allowed. Each time an interaction occurs, one is added to the edge weight. Self-loops were regarded as non-informative and discarded. These networks are reported in literature as exhibiting scale-free and small world properties, as expected for (some) social networks^{10,20}.

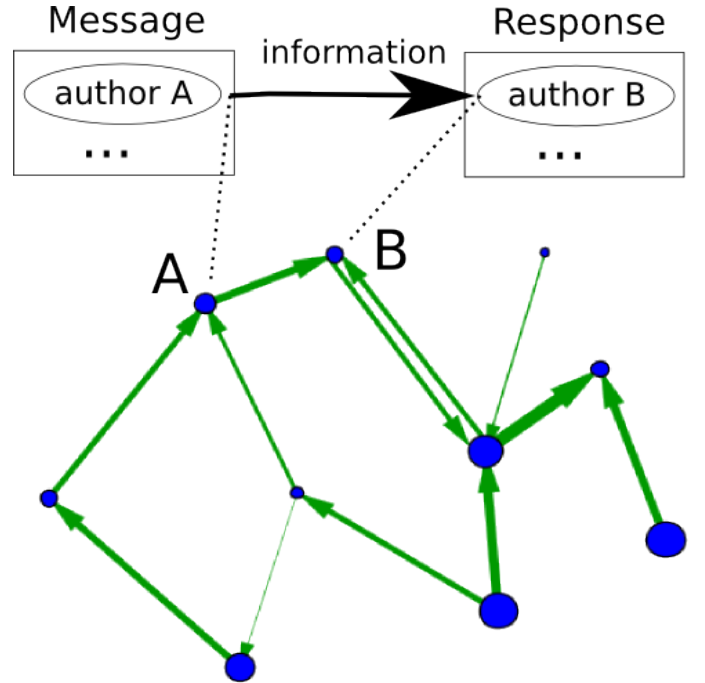


FIG. 1. Formation of interaction network from email messages. Each vertex represents a participant. A reply message from participant B to a message from participant A is regarded as evidence that B received information from A. Multiple messages add “weight” to a directed edge. Further details are given in Section III B.

Edges can be created from all antecedent messages on the message-response thread. We only linked the immediate antecedent to the new message’s author, both for simplicity and for the valid objection that in adding two edges, $x \rightarrow y$ and $y \rightarrow z$, there is also a weaker connection between x and z . Potential interpretations for this weaker connection are: double length, half weight or with one more “obstacles”. This suggests pertinence of centrality measures that account for the connectivity with all nodes, such as betweenness centrality and accessibility^{21,22}.

1. Sectioning networks in periphery, intermediary and hubs sectors

Social networks tend to have a scale-free distribution of connectivity, and the primitive sectors (periphery, intermediary and hubs) can be derived from comparison with an Erdős-Rényi network with the same number of edges and vertices²³, as depicted in Figure 2. The degree distribution $\tilde{P}(k)$ of an ideal scale-free network \mathcal{N}_f with N vertices and z edges has less average degree nodes than the distribution $P(k)$ of an Erdős-Rényi network with the same number of vertices and edges. Indeed, we define in this work the intermediary sector of a network to be the set of all the nodes whose degree is less abundant in the real network than on the Erdős-Rényi model:

$$\tilde{P}(k) < P(k) \Rightarrow k \text{ is intermediary degree} \quad (1)$$

If \mathcal{N}_f is directed and has no self-loops, the probability of an edge between two arbitrary vertices is $p_e = \frac{z}{N(N-1)}$ (see Appendix A). A vertex in the ideal Erdős-Rényi digraph with the same number of vertices and edges, and thus the same probability p_e for the presence of an edge, will have degree k with probability:

$$P(k) = \binom{2(N-1)}{k} p_e^k (1-p_e)^{2(N-1)-k} \quad (2)$$

The lower degree fat tail represents the border vertices, i.e. the peripheral sector or periphery where $\tilde{P}(k) > P(k)$ and k is lower and any intermediary sector value of k . The higher degree fat tail is the hub sector, i.e. $\tilde{P}(k) > P(k)$ and k is higher than any intermediary sector value of k . The reasoning for this classification is: 1) vertices so connected that they are virtually inexistent in networks connected at pure chance (e.g. without preferential attachment) are correctly associated to the hubs sector. Vertices with very few connections, which are way more abundant than expected by pure chance, are assigned to the periphery. Vertices with degree values predicted as the most abundant if connections are created by pure chance, near the average, and less frequent in scale-free phenomena, are classified as intermediary.

To ensure statistical validity, bins can be chosen to contain at least η vertices. Thus, each bin, starting at degree k_i , spans $\Delta_i = [k_i, k_j]$ degree values, where j is the smallest integer with which there are at least η vertices with degree larger than or equal k_i , and less than or equal k_j . This changes equation 1 to:

$$\sum_{x=k_i}^{k_j} \tilde{P}(x) < \sum_{x=k_i}^{k_j} P(x) \Rightarrow i \text{ is intermediary} \quad (3)$$

If strength s is used for comparison, P remains the same, but $P(\kappa_i)$ with $\kappa_i = \frac{s_i}{\bar{w}}$ should be used for comparison, with $\bar{w} = 2 \frac{z}{\sum_i s_i}$ the average weight of an edge and

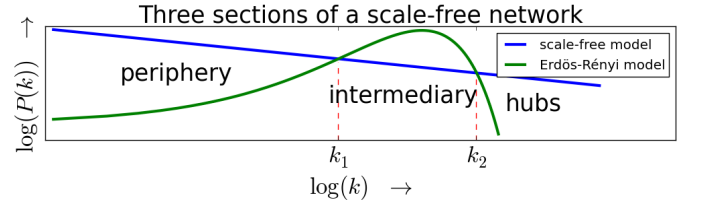


FIG. 2. Degree distribution on scale-free and Erdős-Rényi ideal networks. The latter has more intermediary vertices, while the former has more peripheral and hub vertices. Sector borders are given by the two intersections k_1 and k_2 of the connectivity distributions. Characteristic degrees are in compact intervals of degree: $[0, k_1]$, $(k_1, k_2]$, $(k_2, k_{max}]$ for the three sectors considered (periphery, intermediary and hubs).

s_i the strength of vertex i . For in and out degrees and strengths, comparison should be made with $\kappa_i = 2k_i^{in}$, $\kappa_i = 2k_i^{out}$, $\kappa_i = 2 \frac{s_i^{in}}{\bar{w}}$ and $\kappa_i = 2 \frac{s_i^{out}}{\bar{w}}$. Results of these criteria for network segmentation are discussed in Section IV B and exhibited in Figures 6 to 33 of Appendix D.

Since different metrics can be used in the segmentation to identify the three types of vertices, various criteria can be defined, e.g. with a very stringent criterion according to which a vertex will only be classified as hub if it is so for all the metrics. After a careful inspection of possible combinations, these were reduced to six:

- **Exclusivist criterion:** vertices are only classified if the class is the same according to all metrics. In this case, vertices classified (usually) does not reach 100%, which is indicated by a black line in the figures of Appendix D.
- **Inclusivist criterion:** a vertex has the class given by any of the metrics. Therefore, a vertex can belong to more than one class, and the percentages of members may add to more than 100%, which is indicated by a black line in the figures of Appendix D.
- **Exclusivist cascade:** vertices are only classified as hubs if they are hubs according to all metrics. Intermediary are the vertices classified either as intermediary or hubs with respect to all metrics. The remaining vertices are regarded as peripheral.
- **Inclusivist cascade:** vertices are hubs if they are so classified according to any of the metrics. The remaining vertices are classified as intermediary, if they belong to this category for any of the metrics. Peripheral vertices will then be those which were not classified as hub or intermediary with any of the metrics.
- **Exclusivist externals:** vertices are only hubs if they are classified as such according to all the metrics. The remaining vertices are classified as peripheral if they fall into the periphery or hub classes by any metric. The rest of the nodes are classified as intermediary.

- Inclusive external: hubs are vertices classified as hubs according to any metric. The remaining vertices will be peripheral if they are classified as such according to any metric. The rest of the vertices will be intermediary vertices.

These compound criteria, and the simplification of possibilities listed above (exclusivist/inclusivist, criterion/cascade/externals), can be formalized in strict mathematical terms, but this was considered out of the scope of the present article. Important here is to notice that the compound criteria can be used to examine network sections in the case of a low number of messages, such as in the last figures of Appendix D.

Results from applying this classification method, i.e. the achievement of well defined sectors by comparison of the real network with the Erdős Rényi model, are reported in Section IV B and Appendix D.

2. Topological measurements

The topology of the networks was characterized with a small selection of the most standard measurements for each vertex, as follows:

- Degree k_i : number edges linked to vertex i .
- In-degree k_i^{in} : number of edges ending at vertex i .
- Out-degree k_i^{out} : number of edges departing from vertex i .
- Strength s : sum of weights of all edges linked to vertex i .
- In-strength s_i^{in} : sum of weights of all edges ending at vertex i .
- Out-strength s_i^{out} : sum of weights of all edges departing from vertex i .
- Clustering coefficient cc_i : fraction of pairs of neighbors of i that are linked. The standard clustering coefficient for undirected graphs was used.
- Betweenness centrality bt_i : fraction of geodesics that contain the vertex i . Betweenness centrality index considered directions and weight, as specified in²⁴.

In order to capture symmetries in the activity of participants, the following metrics were introduced for a vertex i (see Section IV C):

- Asymmetry: $asy_i = \frac{d_i^{in} - d_i^{out}}{d_i}$.
- Mean of asymmetry of edges: $\mu_i^{asy} = \frac{\sum_{j \in J_i} e_{ji} - e_{ij}}{|J_i|}$. Where e_{xy} is 1 if there is an edge from x to y , 0 otherwise. $|J_i|$ is the number of neighbors of vertex i .

- Standard deviation of asymmetry of edges: $\sigma_i^{asy} = \sqrt{\frac{\sum_{j \in J_i} [\mu_{asy} - (e_{ji} - e_{ij})]^2}{|J_i|}}$
- Disequilibrium: $dis_i = \frac{s_i^{in} - s_i^{out}}{s_i}$.
- Mean of disequilibrium of edges: $\mu_i^{dis} = \frac{\sum_{j \in J_i} \frac{w_{ji} - w_{ij}}{s_i}}{|J_i|}$, where w_{xy} is the weight of edge $x \rightarrow y$ and zero if there is no such edge.
- Standard deviation of disequilibrium of edges: $\sigma_i^{dis} = \sqrt{\frac{\sum_{j \in J_i} [\mu_{dis} - \frac{(w_{ji} - w_{ij})}{s_i}]^2}{|J_i|}}$

C. Evolution of the networks

The evolution of the networks was observed within a fixed number of messages, the window size ws , that shifts in the message timeline. The ws used were 50, 100, 200, 400, 500, 800, 1000, 2000, 2500, 5000 and 10000. Within a same ws , the number of vertices and edges vary in time, as do other network characteristics.

D. Visualization of network evolution

The evolution of the networks was visualized with animations, image galleries and online gadgets made for this research²⁵⁻²⁷. Such visualizations were crucial to guide research into the most important features of network evolution, and prompted us to capture the prominence of topological metrics along time using mean and standard deviations (see Section IIIB 2 and Appendix C 1), in addition to the size of the three sectors in a timeline fashion (Appendix D). Visualization of network structure was specially useful as part of the email lists data mining, from which parts of relevant structures and results were driven. See Appendix IA for further directions about visualization and text mining concerning the results herein presented, with dedicated articles.

E. Topological deepening

There are other ways to split and characterize networks. To point a common example, the center of the network is defined as all the nodes whose maximum distance to any other node is the radius (the radius is the minimum maximum distance to all vertices, i.e. the radius is the minimum eccentricity). In the same framework, the periphery (as opposed to the center) consists of the nodes whose maximum distance to any node is the diameter (diameter being the maximum geodesic on the network). Accordingly, the intermediary sector can be defined as the nodes that are not in the center or in the periphery. Interestingly, in the email networks analyzed,

with such criteria, the center can often be a factor of 4 times larger than the periphery and the intermediary group often exceeds 90% of the nodes²⁸.

Models of human dynamics can be used to predict and classify activity. In this case, agent activity is commonly considered a Poisson process, as a consequence of the randomly distributed events in time. Even so, evidence-based models suggests that human activity patterns follow non-Poisson statistics, characterized by a long tail of inactivity with bursts of rapidly occurring events^{29,30}. Emails are reported as having a heavy tailed distribution with $\alpha = 1$, together with web browsing and library loans²⁹.

Typologies can also be conveniently adapted from psychiatric, psychological and psychoanalytic theories. Concerning empirical research, Theodor Adorno is a core conceiver of an one-of-a-kind typology that resulted from observing authoritarian personality traces to detect Nazism adoption, antisemitism and potential fascists, depicted as an authoritarian syndrome³¹.

Other classic typologies of interest include Jung's extroversion-introversion trait with four modes of orientation. This four modes are divided in two perceiving functions (sensation and intuition) and two judging functions (thinking and feeling), each individual manifesting one of these four modes as dominant, and each mode expressed primarily as introverted or extroverted³². Myers-Briggs Type Indicator extrapolated Jungian theories into a questionnaire and added perceiving and judging as a fourth dipole³³. Even plain Freudian criteria, such as neurosis, psychosis, perversity and denegation, can be used directly for such categorization, as they have verbal and behavioral typical traces^{34,35}.

It was considered central to benefit from key human typologies, both by describing types and by further characterizing classes in the terms encountered. A primitive physics-based typology is described in Section IV D as a consequence of the periphery, intermediary and hub sectors yielded by comparing the real networks with the Erdős Rényi model. Also, ethic and moral issues are developed by such legacy. For example, Adorno et al. conceptualized that personality is dynamic, not static or immutable, and that recognizing this was important for an ethic empirical study of human authoritarian traces³¹. Indeed, this dynamic typological approach is so vital to secure an ethic study of human systems that our epigraph is devoted to make this point explicit.

IV. RESULTS AND DISCUSSION

Remarkable features from the analysis of the four email lists are:

- The activity along time is practically the same for all lists (Section IV A).
- The fraction of participants in each connective sector is stable and can be observed even with very

few messages (Section IV B).

- The measures combine in principal components in the same way and with symmetry related measures presenting more dispersion than clustering coefficient (Section IV C).
- Typology speculations are immediate from results (Section IV D).

Furthermore, the Appendix holds tables and figures from which such results can be observed.

A. Constancy and discrepancy of activity along time

One remarkable feature from the analysis is that the activity along time is practically the same for all lists.

1. Seconds and minutes

The incidence of messages at each second of a minute and at each minute of an hour is compatible with uniform distribution simulations³⁶. Messages were slightly more evenly distributed in all lists: for both seconds and minutes $\frac{\max(\text{incidence})}{\min(\text{incidence})} \in (1.26, 1.275]$. Simulations reach these values but have in average more discrepant higher and lower peaks $\xi = \frac{\max(\text{incidence}')}{\min(\text{incidence}')} \Rightarrow \mu_\xi = 1.2918$ and $\sigma_\xi = 0.04619$.

2. Hours of the day

Higher activity was observed between noon and 6pm, followed by the time period between 6pm and midnight. Around 2/3 of the whole activity takes place from noon to midnight, as can be seen in Table VI. Nevertheless, the activity peak occurs around midday, with a slight skew toward one hour before noon.

3. Days of the week

Higher activity was observed during weekdays, specially for the CPP and MET lists (see Table VII). The decrease of activity on weekends reaches at least one third, and two thirds in extreme cases.

4. Days along the month

Table VIII shows activity along the month. Variation of activity in the days along the month is less prominent, one cannot point much more than a - probably not statistically relevant - tendency of first and second weeks to be more active. The most important trait seems to be homogeneity. Last days of the month (29, 30 and 31)

are not present in every month, and observed activity is proportional to incidence rates.

5. Months and larger divisions of the year

Activity is concentrated in Jun-Aug for MET and LAD, and in Dec-Mar for CPP, LAU and LAD (see Table IX). These observations fit academic calendars, vacations and end-of-year holidays.

B. Scalable fat-tail structure: constancy of participants fraction in the connective sectors

There is a concentration of hub activity and of vertex with few connections. Table V is dedicated to exposing this well known and expected distribution of activity among participants.

The distribution of vertices in the three sectors defined in Section IIIB 1 (hubs, intermediary, periphery) is remarkably stable along time, provided that a sufficiently large sample of 200 or more messages is considered. Moreover, the same distribution applies to the networks of all the four email lists, to which are dedicated the various figures in Appendix D. If, for instance, strength is taken as the criterion to define the sectors, $\approx 5\%$ of the vertices are found to be hubs, $\approx [15 - 20]\%$ are intermediary and $\approx [75 - 80]\%$ are peripheral, which is consistent with the literature³⁷. If the degree is used for classification, hubs can reach 10% of all vertices, i.e. classification with strength yields half the number of hubs as plain degree. These results hold for in and out degrees and strengths. Stable distributions can also be obtained for 200 or less messages if classification of the three sectors is performed with one of the compound criteria established in Section IIIB 1. In fact, a minimum window size for observation of more general properties can be inferred by monitoring the giant component and the degeneration of the hub, intermediary and peripheral sections. This degeneration is critical in the span of 50-100 messages. Even so, using a compound criterion, such as exclusive cascade of Figure 15, the networks seem to hold their basic structure with as few as 20-50 messages. This indicates that concentration of activity and the abundance of low-activity participants take place even with very few messages, which is highlighted in the last figures of Appendix D.

For the histograms used in the classification process (see Section IIIB 1), the use of at least η vertices for each bin did not yield significant differences. That was understood as a consequence of the observation scale: *There are between 20 and 200 participants in the message window sizes used to derive most of the results ($ws \in [200, 1500]$ messages). As peripheral vertices are abundant and span few degrees, there are more than η vertices with each low degree value. For the case of higher degrees, one should consider that with the ws used, each*

participant is $p \in [0.1\%, 0.5\%]$ of all participants. Therefore, if incident connectivity is very improbable in an Erdős Rényi network (less than p , the probability that a single participant represents when the histogram is normalized to the density function), then it is not an intermediary connectivity, but a hub. Therefore, using at least η vertices for each bin did not impact the results.

C. Prevalence of centrality over symmetry and symmetry over clusterization

The contribution from the distinct metrics to network topology is very similar for all the networks considered, and did not vary with time. This stability in network behavior is remarkable, as can be noticed by the very small standard deviations of the contributions from the metrics along time (Tables II-IV).

The principal component (PCA³⁸) exhibited a ponderation of centrality measures: degrees, strengths and betweenness centrality. Clustering coefficient is presented in almost perfect orthogonality. Symmetry of edges have been reported as bonded to different roles played by participants and relations², and dispersion was more prevalent in symmetry related measures than clustering coefficient. This composition of the principal component suggests that all six degree and strength measures are equally important for system characterization, although it is known that they do not relate to the same participation characteristics. The contribution from the distinct metrics to network topology variance is very similar for all the networks considered, and did not vary with time. This stability in network behavior is remarkable, as shown by the very small standard deviations of the contributions from the metrics along time in Appendix C 1.

The dispersion is mostly presented by degree, strength and betweenness centrality, as indicated in Tables II and III for the LAU list (similar results are obtained for the other lists and omitted here for simplicity). The standard deviations are small, which means that the first and second components varies little with time. Degree and strength are highly correlated, with Spearman correlation coefficient $\in [0.95, 1]$ and Pearson coefficient $\in [0.85, 1]$ for $ws > 1000$. The corresponding PCA plot for the two first components is shown in Figure 3, where each vertex is colored according to the sector they belong. As expected, peripheral vertices have very low values in the first component and greater dispersion in the second component. The plot of clustering coefficient versus degree in Figure 4 is similar to the PCA in Figure 3.

The PCA plot in Figure 5, where all metrics are considered, reflects symmetry-related relevance for the variance. This is shown in Table IV where the clustering coefficient is only relevant for the third principal component (with contributions from out-degree and out-strength). It is concluded that the symmetry-related measurements can be more meaningful in characterizing interaction networks (and their participants) than the clustering co-

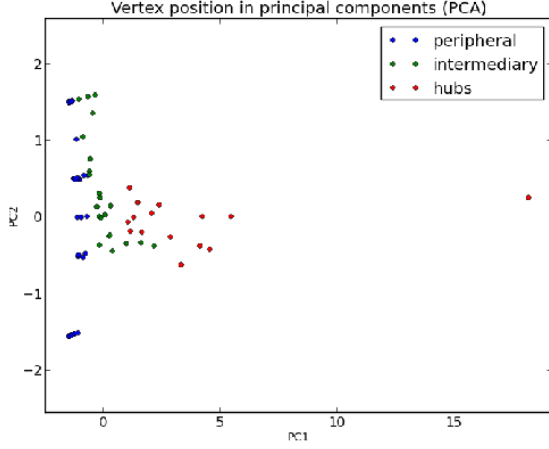


FIG. 3. Scatter plot of vertices for the LAU list using two principal components from a PCA in the metrics space of in- and out- degree and strength, betweenness centrality and clustering coefficient, as specified in Section III B 2. Principal component is a weighted average of centrality measures: degrees, strengths and betweenness centrality. Second component is mostly clustering coefficient. Table III shows the composition of principal components. Similar plots were obtained for all window sizes $ws \in [500, 10000]$, and for the networks of the other email lists, which exposes a common relation held by degree, strength and betweenness measures to clustering coefficient.

efficient, especially for hubs and intermediary vertices, which are more dispersed in Figure 5 than in Figure 3.

D. Primitive typology: the activity of participants from different sectors

This work is aimed at finding common characteristics among (email) interaction networks. Analysis involved primary measures observance and a formal criteria for coherent ratios of hub, intermediary and hub sectors. In this process, inspection done by visualizations and raw data manipulations suggests agents typological peculiarities. These are initial observations, which inspired this article and other ongoing research:

- Core hubs usually have intermittent activity. Very stable activity was found on MET hubs, which motivated its integration to this work. There are reports in the literature of greater stability of participation in smaller communities¹, which is the reason why the smaller number of participants in MET was considered coherent with the stable activity of hubs.
- Typically, the activity of hubs is trivial: they interact as much as possible, in every occasion with everyone. The activity of peripheral vertices also follows a simple pattern: they interact very rarely,

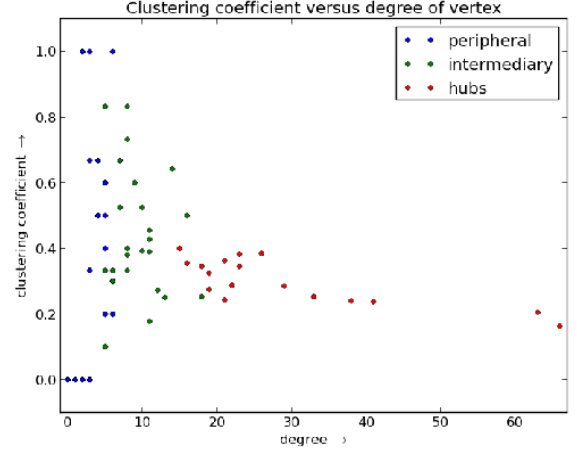


FIG. 4. Clustering coefficient versus degree of vertices with a window size of $ws = 1000$ email messages, LAU list. The general layout is consistent with the literature: most connected vertices have low clusterization while higher clusterization is gradually more incident as the number of connections is lowered.

in very few occasions. Therefore, intermediary vertices seem responsible for the network structure. For example, intermediary vertices may exhibit preferential communication to peripheral, intermediary, or hub vertices; can be marked by stable communication partners; can involve stable or intermittent patterns of activity.

- Some of the most active participants receive many responses with relative few messages sent, and rarely are top hubs. These seem as authorities and contrast with participants that respond much more than receive responses.
- The most obvious community structure, as observed by high clustering coefficient, is found only in peripheral and intermediary sectors.

This “primitive typology”, characterized by peripheral, intermediary and hub types, can be further scrutinized using concepts involved in other typologies, such Meyer-Briggs, Pavlov or F-Scale. This has no pretension of being a direct result of numeric analysis, it is a description refinement of the found structure, in typological terms, and coherent with complex networks literature. Although initial, this bridges human and exact sciences in the most pertinent way authors were able to, as is herein considered a result.

Another typology suggested by results is about the networks themselves. In accordance with previous research results¹, this and paired articles^{6,11} reports a dipole in human interaction network types: networks with few and stable agents, and (relative) many threads per amount of messages contrasts with networks with many agents of intermittent activity and (relative) few threads per amount

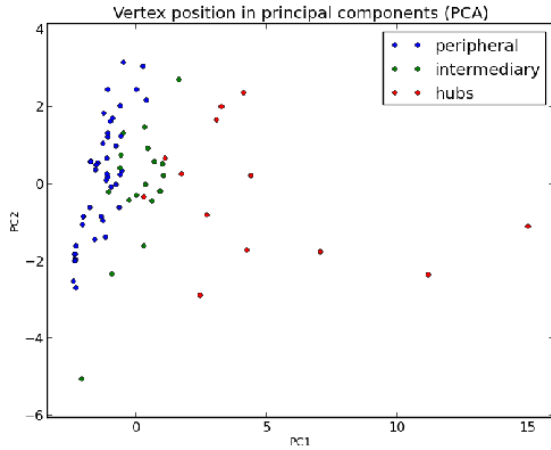


FIG. 5. Scatter plot of vertices for the LAU list using two principal components from a PCA in the metrics space of (in-, out- and total) degree, (in-, out- and total) strength, betweenness centrality, clustering coefficient and symmetry-related measurements. The composition of the first three components are shown in Table IV and measure details in Section III B 2. Most importantly, clustering coefficient is only relevant for third component, being second component representative of symmetry measurements of vertex interactions. Dispersion suggests symmetry related measures are more powerful for characterizing interaction networks than clustering coefficient, specially for hubs and intermediary vertices.

of messages.

V. CONCLUSIONS AND FURTHER WORK

The characterization of interaction networks resulted from stability observations. Along temporal activity statistics, this work reports the stability of the principal components (in the concentration of dispersion and composition) and of the ternary partitioning (periphery, intermediary, hubs) relative sizes, evident in the comparison with the Erdős-Rényi model. These results suggested typologies for both agents and the networks.

The task of delivering a first and general characterization of chosen interaction networks involved a larger effort. The different aspects covered requires not only different analytical background, but also considerations about textual production and social psychology. These are receiving attention within dedicated works and are summarized in Section I A.

Regarding topological aspects of interaction networks, further work should inspect other measures in each of the three connective sectors: hubs, intermediary and periphery. Observance of attributes with greater contribution to principal components of LDA should reveal best chances to present these three sections as clusters in the network measurements space. Another possibility, spe-

cially for a brute-force characterization of such sectors, is to remove vertices with degree close to k_1 or k_2 depicted in figure 2. The subtraction $\tilde{P}(k) - P(k)$ (see Section III E) results in two positive clusters for periphery and hubs, and a negative cluster for intermediary vertices. This might support classification of the three sectors by clustering, a more traditional approach to classification.

Observed networks were coherent with literature in different aspects, such as concentration of activity, and clusterization versus connectivity patterns. Even so, analysis of data from other virtual environments, such as Facebook, Twitter and LinkedIn, might help understanding how general are these structures and what are proper uses.

A. Results exploitation

A paired article is dedicated to textual production of the network sectors⁶. Resulting knowledge purposes networks and participants typologies, and both topological and textual analysis should foster characterization of interaction networks and participation incidences. Stability reported in this article eases tipologization of outliers and more usual participation patterns (see Sections I A and IV D).

On the technological trend, usage of such characteristics are taking place in linked data and electronic government technologies^{39–41}. Further steps involve elaboration and tests of social dynamics. These results are also being used for anthropological physics experiments⁴².

ACKNOWLEDGMENTS

Renato Fabbri is grateful to CNPq (process: 140860/2013-4, project 870336/1997-5), United Nations Development Program (PNUD/ONU, contract: 2013/000566; project BRA/12/018) and the Postgraduate Committee of the IFSC/USP. This author is also grateful for the American Jewish Committee for maintaining an online copy of the Adorno book used on the epigraph³¹. Authors thank GMANE creators and maintainers, specifically: GMANE is run by Lars Magne Ingebrigtsen, and the administrators are Tom Koelman, Jason R. Mastaler, Steinar Bang, Jon Ericson, Wolfgang Schnerring, Sebastian D.B. Krause, Nicolas Bareil, Raymond Scholz, and Adam Sjgren. Authors thank referred email lists communities and welcome feedback as core contribution to this, and similar, research.

Appendix A: Edge existence probability in a directed network without self-loops

Be \mathcal{N} a directed network without self-loops with z edges and N vertices. The probability

that an edge exists between two arbitrary vertex is $p_e = \frac{z}{\max(\text{number of edges} \mid N \text{ vertices})}$, where $\max(\text{number of edges} \mid N \text{ vertices}) = 2[(N-1) + (N-2) + \dots + 1] = 2[\sum_{i=1}^{N-1} i] = 2[\frac{N(N-1)}{2}]$ is the maximum number of edges for a network with N vertices. Therefore:

$$\begin{aligned} p_e &= \frac{z}{\max(\text{number of edges} \mid N \text{ vertices})} \\ &= \frac{z}{2[(N-1) + (N-2) + \dots + 1]} = \frac{z}{2 \frac{N(N-1)}{2}} \\ p_e &= \frac{z}{N(N-1)} \end{aligned} \quad (\text{A1})$$

Appendix B: Data and scripts

Messages are downloaded from the GMANE database by RSS in the mbox email text format. They are requested one by one to avoid reaching maximum size of the requests accepted by GMANE API.

Every message has about 30 fields, from which the following are crucial for the present work:

- “From” field, as it specifies the sender of the message, in the usual format of “First_name Last_Name <email>”.
- “Date” field, which is given with the resolution of a second.
- “Message-ID”, important to state antecedent/consequent relation between messages and therefore from an author to a replier.
- “References”, has the ID of the message it is an answer to, if any, and earlier messages in the thread.

Field “In-Reply-To” has only the ID of the message it replies and can be sometimes a shortcut or an alternative to “References”. Also, the textual content of the messages, accessed through “payload” method of the mbox message object, is of central interest and the authors dedicated an article to include the textual content of the messages to the analysis⁶.

1. Python scripts

Basic constructs for obtaining all results are the product of scripts written in the Python programming language. These are kept in a public git repository for backup and sharing with research community⁴⁸. Core scripts, for deriving structures and results exhibited in this article, are in the LEIAME file.

2. Third party libraries and software

The programming framework used is mainly Python-based, with emphasis on usual scientific tools. More

specifically, scripts were written for 2.7.3 version of Python, with the following third party libraries: Numpy, Pylab/Matplotlib, NetworkX, IGraph. Behind the scenes, Graphviz is accessed via PyGraphviz to make network drawings.

Appendix C: Tables

1. PCA tables

TABLE II. Principal components composition in the simplest case: with degree, clustering coefficient and betweenness centrality. LAU list, $ws = 1000$ messages in 20 disjoint positioning was used for statistics. The first component is a weighted average of degree and betweenness centrality. The second component is mostly clustering coefficient. The first and second components represent more than 95% of total variance. The λ bottom line holds the percentage of total variance attributed to each component.

	PC1		PC2		PC3	
	μ	σ	μ	σ	μ	σ
d	48.02	1.39	2.82	1.74	48.09	0.32
cc	4.12	2.94	90.45	3.98	3.98	0.77
bt	47.87	1.55	6.74	4.08	47.93	0.46
λ	64.67	0.52	33.26	0.23	2.08	0.40

TABLE III. Principal components composition in percentages. LAU list, $ws = 1000$ messages in 20 disjoint positioning was used for statistics. First component is a weighted average of degree and strength and betweenness centrality. The second component is mostly related to the clustering coefficient. The first and second components represent more than 90% of the variance.

	PC1		PC2		PC3	
	μ	σ	μ	σ	μ	σ
d	14.58	0.14	0.43	0.35	1.51	1.08
d^{in}	14.12	0.14	1.71	1.22	17.80	6.20
d^{out}	13.95	0.12	2.80	1.83	21.15	5.62
s	14.48	0.13	0.78	0.65	5.51	4.71
s^{in}	14.10	0.14	2.17	1.28	17.32	6.11
s^{out}	14.05	0.13	2.08	1.14	19.31	4.86
cc	0.99	0.70	83.38	4.83	2.75	1.62
bt	13.73	0.19	6.65	1.31	14.66	10.14
λ	81.80	0.83	12.53	0.09	3.24	0.62

TABLE IV. Principal components formation with symmetry-related metrics (see Section III B 2). LAU list, $ws = 1000$ messages in 20 disjoint positioning was used for statistics. In this case, clusterization is pushed to the third principal component. The second component is primarily derived from symmetry measurements, but also out-degree and out-strength, and disequilibrium standard deviation. Betweenness centrality again has a role similar to degree, but weaker. The clusterization component combines with disequilibrium, while asymmetry is combined to out-degree and out-strength. The three components have in average 80.36% of the variance.

	PC1		PC2		PC3	
	μ	σ	μ	σ	μ	σ
d	11.51	0.42	2.00	0.76	2.39	0.49
d^{in}	11.45	0.34	2.86	0.91	1.68	0.67
d^{out}	10.68	0.60	7.43	1.00	3.00	1.02
s	11.37	0.42	1.75	0.71	4.31	0.63
s^{in}	11.33	0.35	2.39	1.10	3.69	0.86
s^{out}	10.74	0.55	6.14	1.05	4.75	0.98
cc	0.91	0.64	2.68	1.67	22.27	6.43
bt	10.87	0.38	1.17	0.93	4.03	1.42
asy	3.99	1.45	18.13	1.67	2.55	1.77
μ_{asy}	4.15	1.40	17.07	1.78	2.49	1.67
σ_{asy}	1.21	0.67	17.49	0.79	3.29	2.33
dis	5.78	0.51	1.94	1.28	24.75	3.73
μ_{dis}	0.79	0.49	14.00	1.14	3.73	3.13
σ_{dis}	5.18	0.72	4.93	2.48	17.04	4.78
λ	51.09	1.07	20.04	1.31	9.23	6.63

TABLE V. Distribution of activity among agents. First column is dedicated to percentage of messages sent by the most active participant. Column for the first quartile ($1Q$) exhibits minimum percentage of participants responsible for at least 25% of total messages. Similarly, the column for the first three quartiles $1 - 3Q$ exhibits minimum percentage of participants responsible for 75% of total messages. The last decile $10D$ column has maximum percentage of participants responsible for 10% of messages.

list	hub	$1Q$	$1 - 3Q$	$10D$
CPP	14.41	0.19 (27.8%)	4.09 (75.13%)	83.65 (-10.04%)
MET	11.14	0.81 (30.61%)	8.33 (75.11%)	80.49 (-10.02%)
LAU	2.78	1.10 (25.16%)	13.02 (75.04%)	67.37 (-10.03%)
LAD	4.00	0.95 (25.50%)	11.83 (75.07%)	71.13 (-10.03%)

2. Tables for activity along time and among participants

TABLE VI. Percentage of activity ($100 \frac{\text{counted messages}}{\text{total messages}}$) in each hour, 6 hours and 12 hours. Maximum activity rates are in bold. In 1h columns, minimum activity is also bold. The less active period of the day is around 4-6h. Maximum activity is between 10-13h. Afternoon is most active in 6h division of the day. The noon has $\approx \frac{2}{3}$ of 24h activity.

	CPP			MET			LAU			LAD		
	1h	6h	12h	1h	6h	12h	1h	6h	12h	1h	6h	12h
0h	3.66	10.67	33.76	2.87	7.15	29.33	3.58	10.14	36.88	4.00	10.77	33.13
1h	2.76			1.77			2.22			2.52		
2h	1.79			1.04			1.63			1.79		
3h	1.10			0.64			1.06			1.06		
4h	0.68	23.09	33.76	0.47	22.18	29.33	0.84	26.74	36.88	0.75	22.36	33.13
5h	0.69			0.38			0.82			0.66		
6h	0.83			0.72			1.17			0.85		
7h	1.24			1.33			2.37			1.56		
8h	2.28	28.61	66.24	2.67	28.44	70.66	3.54	27.46	63.12	2.96	29.63	66.87
9h	4.52			4.40			6.04			4.68		
10h	6.62			6.29			6.83			5.93		
11h	7.61			6.78			6.79			6.40		
12h	6.44	37.63	66.24	7.33	42.22	70.66	6.11	35.65	63.12	6.41	37.25	66.87
13h	6.04			7.08			6.26			6.12		
14h	6.47			7.09			6.38			6.33		
15h	6.10			7.14			5.93			5.98		
16h	6.22	28.61	66.24	6.68	28.44	70.66	5.52	27.46	63.12	6.40	29.63	66.87
17h	6.36			6.89			5.46			6.02		
18h	6.01			5.99			5.24			5.99		
19h	5.02			5.23			4.52			5.03		
20h	4.85	28.61	66.24	4.98	28.44	70.66	4.55	27.46	63.12	4.63	29.63	66.87
21h	4.38			4.37			4.42			4.59		
22h	4.06			4.24			4.51			4.88		
23h	4.30			3.64			4.23			4.53		

TABLE VII. Percentage of activity on days along the week. Weekend days are at least $\frac{1}{3}$ less active and can reach $\frac{1}{3}$ of activity. MET concentrates activity in weekdays the most, leaving only 13.98% of total activity to Saturday and Sunday. LAU is the one that less concentrates activity in weekdays, reaching 20.94% of total activity in weekends. These might suggest professional relation of CPP and MET participants to the topics of interest, or a hobby relation of LAU and LAD participants.

	Mon	Tue	Wed	Thu	Fri	Sat	Sun
CPP	17.06	17.43	17.61	17.13	16.30	6.81	7.67
MET	17.53	17.54	16.43	17.06	17.46	7.92	6.06
LAU	15.71	15.80	15.88	16.43	15.13	10.13	10.91
LAD	14.91	17.73	17.01	15.40	14.25	10.39	10.30

TABLE VIII. Activity along the days of the month. The pattern is to have no clear prevalent period. One might point a slight tendency for the first two weeks to be more active, although this table does not present statistical foundation for such an assumption. For the scope of this study, differences of activity along the month is assumed to be inexistent.

	CPP			MET			LAU			LAD		
day	1 day	7 days	14 days	1 day	7 days	14 days	1 day	7 days	14 days	1 day	7 days	14 days
1	3.19			3.01			3.34			3.22		
2	3.07			3.38			3.38			3.42		
3	3.20			3.55			3.20			2.87		
4	3.63	23.05		4.34	25.16		3.52	23.06		2.91	21.96	
5	2.85			3.93			2.68			3.30		
6	3.67			3.76			3.18			3.52		
7	3.45		45.63	3.18		48.08	3.77		47.31	2.27		
8	3.12			3.36			3.62			3.72		46.70
9	2.57			3.44			3.82			3.97		
10	2.92			3.17			3.06			3.77		
11	3.54	22.57		3.88	22.92		3.11	24.25		3.27	24.73	
12	3.23			2.94			3.40			2.75		
13	3.39			3.29			3.55			3.34		
14	3.81			2.83			3.69			3.93		
15	3.35			2.72			3.23			3.37		
16	3.77			2.96			2.94			3.37		
17	3.45			3.01			3.02			2.95		
18	3.47	23.02		3.39	21.87		3.63	22.84		3.22	22.82	
19	2.90			3.42			3.16			3.59		
20	2.80			3.09			3.25			3.21		
21	3.29		46.31	3.27		43.56	3.61		44.01	3.13		46.00
22	2.88			2.92			3.80			3.07		
23	4.01			3.27			3.03			3.06		
24	3.13			2.92			2.31			2.72		
25	3.57	23.29		2.83	21.69		2.38	21.17		3.16	23.18	
26	3.27			2.97			3.49			3.57		
27	3.27			3.41			2.92			3.92		
28	3.17			3.36			3.26			3.69		
29	3.68			2.93			3.34			3.15		
30	2.76	8.06	8.06	3.14	8.36	8.36	3.75	8.68	8.68	2.71	7.30	7.30
31	1.63			2.29			1.60			1.45		

TABLE IX. Activity along the year, in months, trimesters, quadrimesters and semesters. Engagement in list participation seem to concentrate in two periods: middle of the year (Jun-Aug, lists MET and LAD), and transition from years (Dec-Mar, lists CPP, LAU and LAD). Messages were considered as to complete 12 months slots, so every month has the same time of occurrences.

	CPP					MET					LAU					LAD				
	m.	b.	t.	q.	s.	m.	b.	t.	q.	s.	m.	b.	t.	q.	s.	m.	b.	t.	q.	s.
Jan	8.70	17.00	27.23	36.48		4.88	11.01	16.90	23.32		10.22	19.56	28.23	35.09		11.23	18.49	26.43	36.04	
Fev	8.29					6.13					9.34					7.26				
Mar	10.23	19.49			54.26	5.89	12.31			47.74	8.67	15.52		35.09	49.17	7.94	17.55			57.95
Apr	9.26					6.42		30.84			6.85					9.61				
Mai	9.41	17.78	27.03			10.46	24.42				7.27	14.09	20.94			8.94	21.91	31.51		
Jun	8.37			33.46		13.96			47.83		6.81			30.37		12.97			37.56	
Jul	8.70	15.68	22.94			13.23	23.41	31.16			8.96	16.28	24.47			9.02	15.65	22.29		
Ago	6.98					10.28				52.26	7.31					6.63				
Set	7.26	15.36			45.73	7.75	16.80				8.18	16.24			50.82	6.63	12.38			
Oct	8.10					9.05					8.06					5.74				
Nov	7.86		22.80	30.06		7.46		28.86			7.63		26.36	34.54		7.63			26.40	
Dec	6.81	14.69				4.59	12.06				10.66	18.30				6.39	14.02	19.77		

Appendix D: Figures of vertex classification fractions as the network evolves

Two lists are exhibited in this section, CPP and LAD. These structures are very similar in all four lists and laying extensively all figures is redundant. Window sizes of $ws = 10000, 5000, 1000, 500, 250, 100$ and 50 messages were used.

- ¹Gergely Palla, Albert-László Barabási, and Tamás Vicsek, “Quantifying social group evolution,” *Nature* **446**, 664–667 (2007).
- ²Elizabeth A Leicht, Gavin Clarkson, Kerby Shedden, and Mark EJ Newman, “Large-scale structure of time evolving citation networks,” *The European Physical Journal B* **59**, 75–83 (2007).
- ³M. E. J. Newman, “The structure and function of complex networks,” *SIAM REVIEW* **45**, 167–256 (2003).
- ⁴Mark EJ Newman, “Analysis of weighted networks,” *Physical Review E* **70**, 056131 (2004).
- ⁵Kyle Marek-Spartz, Paula Chesley, and Hannah Sande, “Construction of the gmane corpus for examining the diffusion of lexical innovations,” (2012).
- ⁶Renato Fabbri, “A connective differentiation of textual production in interaction networks,” (2013), <http://arxiv.org/abs/1412.7309>.
- ⁷Renato Fabbri, “Participant typologies derived from textual and topological features in interaction networks,” (2013).
- ⁸Patrick Doreian and Frans Stokman, *Evolution of social networks* (Routledge, 2013).
- ⁹Réka Albert and Albert-László Barabási, “Topology of evolving networks: local events and universality,” *Physical review letters* **85**, 5234 (2000).
- ¹⁰Christian Bird, Alex Gourley, Prem Devanbu, Michael Gertz, and Anand Swaminathan, “Mining email social networks,” in *Proceedings of the 2006 international workshop on Mining software repositories* (ACM, 2006) pp. 137–143.
- ¹¹Renato Fabbri, “Versinus: a visualization method for graphs in evolution,” arXiv preprint arXiv:1412.7311(2014).
- ¹²Lars Magne Ingebrigtsen, “Gmane,” (2008).
- ¹³Wikipedia, “Gmane — Wikipedia, the free encyclopedia,”.
- ¹⁴Gmane.linux.audio.users is list ID in GMANE.
- ¹⁵Gmane.linux.audio.devel is list ID in GMANE.
- ¹⁶Gmane.comp.gcc.libstdc++.devel is list ID in GMANE.
- ¹⁷Gmane.politics.organizations.metareciclagem is list ID in GMANE.
- ¹⁸Elizabeth A Leicht and Mark EJ Newman, “Community structure in directed networks,” *Physical review letters* **100**, 118703 (2008).
- ¹⁹MEJ Newman, “Community detection and graph partitioning,” arXiv preprint arXiv:1305.4974(2013).
- ²⁰Mark Newman, *Networks: an introduction* (Oxford University Press, 2010).
- ²¹L da F Costa, Francisco A Rodrigues, Gonzalo Travieso, and PR Villas Boas, “Characterization of complex networks: A survey of measurements,” *Advances in Physics* **56**, 167–242 (2007).
- ²²BAN Travençolo and L da F Costa, “Accessibility in complex networks,” *Physics Letters A* **373**, 89–95 (2008).
- ²³Matthew O. Jackson.
- ²⁴Ulrik Brandes, “A faster algorithm for betweenness centrality*,” *Journal of Mathematical Sociology* **25**, 163–177 (2001).
- ²⁵Renato Fabbri, Luciano da F. Costa, and Osvaldo N. de Oliveira jr, “Video visualizations of email interaction network evolution,” (2013), http://www.youtube.com/watch?v=-t5jxQ8cKxM&list=PLf_EtaMqu3jU-1j4jiiUiymqyVSzIYeh6.
- ²⁶Renato Fabbri, Luciano da F. Costa, and Osvaldo N. de Oliveira jr, “Image gallery of email interaction networks.” (2013), http://hera.ethymos.com.br:1080/redes/python/autoRede/gmane.linux.audio.devel_3000-4200-280/.
- ²⁷Renato Fabbri, Luciano da F. Costa, and Osvaldo N. de Oliveira jr, “Online gadget for making email interaction network images, gml files and measurements.” (2013), <http://hera.ethymos.com.br:1080/redes/python/autoRede/escolheRedes.php>.
- ²⁸NetworkX Developers, “Networkx,” (2010).
- ²⁹Alexei Vázquez, João Gama Oliveira, Zoltán Dezső, Kwang-II Goh, Imre Kondor, and Albert-László Barabási, “Modeling bursts and heavy tails in human dynamics,” *Physical Review E* **73**, 036127 (2006).
- ³⁰Julián Candia, Marta C González, Pu Wang, Timothy Schoenharl, Greg Madey, and Albert-László Barabási, “Uncovering individual and collective human dynamics from mobile phone records,” *Journal of Physics A: Mathematical and Theoretical* **41**, 224015 (2008).
- ³¹Theodor W Adorno, Else Frenkel-Brunswik, Daniel J Levinson, and R Nevitt Sanford, “The authoritarian personality.” (1950).
- ³²Carl Gustav Jung, HG Baynes, and RFC Hull, *Psychological types*, Vol. 4 (Routledge London, UK, 1991).
- ³³Naomi L Quenk, *Essentials of Myers-Briggs type indicator assessment*, Vol. 66 (Wiley. com, 2009).
- ³⁴Sigmund Freud, “Libidinal types.” *The Psychoanalytic Quarterly*(1932).
- ³⁵Hans J Eysenck, “Types of personality: a factorial study of seven hundred neurotics,” *The British Journal of Psychiatry* **90**, 851–861 (1944).
- ³⁶Numpy version 1.6.1, “random.randint” function, was used for simulations.
- ³⁷Stefano Boccaletti, Vito Latora, Yamir Moreno, Martin Chavez, and D-U Hwang, “Complex networks: Structure and dynamics,” *Physics reports* **424**, 175–308 (2006).
- ³⁸Ian Jolliffe, *Principal component analysis* (Wiley Online Library, 2005).
- ³⁹Renato Fabbri, Rodrigo Bandeira de Luna, Ricardo Augusto Poppi Martins, *et al.*, “Social participation ontology: community documentation, enhancements and use examples,” arXiv preprint arXiv:1501.02662(2015).
- ⁴⁰Produto 5 da consultoria PNUD/ONU de Renato Fabbri, <https://github.com/ttm/pnud4/blob/master/latex/produto.pdf?raw=true> BibitemShutNoStop
- ⁴¹Renato Fabbri, “Ensaio sobre o auto-aproveitamento: um relato de investidas naturais na participa\ c {c}\` ao social,” arXiv preprint arXiv:1412.6868(2014).
- ⁴²Renato Fabbri, “What are you and i? [anthropological physics fundamentals],” academia.edu(2015), https://www.academia.edu/10356773/What_are_you_and_I_anthropological_physics_fundamentals_.
- ⁴³Jukka-Pekka Onnela, Samuel Arbesman, Marta C González, Albert-László Barabási, and Nicholas A Christakis, “Geographic constraints on social network groups,” *PLoS one* **6**, e16939 (2011).
- ⁴⁴Tao Jia and Albert-László Barabási, “Control capacity and a random sampling method in exploring controllability of complex networks,” *Scientific reports* **3** (2013).
- ⁴⁵Yang-Yu Liu, Jean-Jacques Slotine, and Albert-László Barabási, “Control centrality and hierarchical structure in complex networks,” *Plos one* **7**, e44459 (2012).
- ⁴⁶Yang-Yu Liu, Jean-Jacques Slotine, and Albert-László Barabási, “Controllability of complex networks,” *Nature* **473**, 167–173 (2011).
- ⁴⁷Vasyl Palchykov, Kimmo Kaski, Janos Kertész, Albert-László Barabási, and Robin IM Dunbar, “Sex differences in intimate relationships,” *Scientific reports* **2** (2012).
- ⁴⁸Renato Fabbri, Luciano da F. Costa, and Osvaldo N. de Oliveira jr, “Scripts used for obtaining results used in this article ..” (2013), sourceforge.net/p/labmacambira/fimDoMundo/ci/master/tree/python/toolkitGMANE/.
- ⁴⁹Renato Fabbri, “Complex networks and natural language processing collection and diffusion of information and goods.” (2014), wiki.nosdigitais.teia.org.br/ARS.

- ⁵⁰James P Bagrow, Dashun Wang, and Albert-Laszlo Barabasi, "Collective response of human populations to large-scale emergencies," *PloS one* **6**, e17680 (2011).
- ⁵¹Gourab Ghoshal, Nicholas Blumm, Zalan Forro, Maximilian Schich, Ginestra Bianconi, Jean-Philippe Bouchaud, and Albert-Laszlo Barabasi, "Dynamics of ranking processes in complex systems," (2012).
- ⁵²Soon-Hyung Yook, Hawoong Jeong, A-L Barabási, and Yuhai Tu, "Weighted evolving networks," *Physical Review Letters* **86**, 5835 (2001).
- ⁵³Dashun Wang, Zhen Wen, Hanghang Tong, Ching-Yung Lin, Chaoming Song, and Albert-László Barabási, "Information spreading in context," in *Proceedings of the 20th international conference on World wide web* (ACM, 2011) pp. 735–744.
- ⁵⁴Nicholas Blumm, Gourab Ghoshal, Zalán Forró, Maximilian Schich, Ginestra Bianconi, Jean-Philippe Bouchaud, and Albert-László Barabási, "Dynamics of ranking processes in complex systems," *Physical Review Letters* **109**, 128701 (2012).
- ⁵⁵Mark EJ Newman, Steven H Strogatz, and Duncan J Watts, "Random graphs with arbitrary degree distributions and their applications," *Physical Review E* **64**, 026118 (2001).
- ⁵⁶Mark EJ Newman, "Random graphs with clustering," *Physical review letters* **103**, 058701 (2009).
- ⁵⁷Aaron Clauset, Cosma Rohilla Shalizi, and Mark EJ Newman, "Power-law distributions in empirical data," *SIAM review* **51**, 661–703 (2009).
- ⁵⁸Mark EJ Newman, "Assortative mixing in networks," *Physical review letters* **89**, 208701 (2002).
- ⁵⁹Mark EJ Newman, "Modularity and community structure in networks," *Proceedings of the National Academy of Sciences* **103**, 8577–8582 (2006).
- ⁶⁰MEJ Newman, "Communities, modules and large-scale structure in networks," *Nature Physics* **8**, 25–31 (2011).
- ⁶¹Aaron Clauset, Cristopher Moore, and Mark EJ Newman, "Hierarchical structure and the prediction of missing links in networks," *Nature* **453**, 98–101 (2008).
- ⁶²MEJ Newman, "Complex systems: A survey," *arXiv preprint arXiv:1112.1440*(2011).
- ⁶³Brian Ball and Mark EJ Newman, "Friendship networks and social status," *arXiv preprint arXiv:1205.6822*(2012).
- ⁶⁴G. Deleuze, *Difference and Repetition* (Continuum, 1968).
- ⁶⁵F. de Saussure, *Course in General Linguistics* (Books LLC, 1916).
- ⁶⁶A. Papoulis S. U. Pillai, *Probability, Random Variables and Stochastic Processes* (McGraw Hill Higher Education, 2002).
- ⁶⁷R. A. Johnson D. W. Wichern, *Applied Multivariate Statistical Analysis* (Prentice Hall, 2007).
- ⁶⁸C. W. Therrien, *Discrete Random Signals and Statistical Signal Processing* (Prentice Hall, 1992).
- ⁶⁹R. O. Duda P. E. Hart D. G. Stork, *Pattern Classification* (Wiley-Interscience, 2000).
- ⁷⁰L. da F. Costa R. M. C. Jr., *Shape Analysis and Classification: Theory and Practice (Image Processing Series)* (CRC Press, 2000).
- ⁷¹D. Papineau, *Philosophy* (Oxford University Press, 2009).
- ⁷²B. Russel, *A History of Western Philosophy* (Simon and Schuster Touchstone, 1967).
- ⁷³F. G. G. Deleuze, *What Is Philosophy?* (Simon and Schuster Touchstone, 1991).

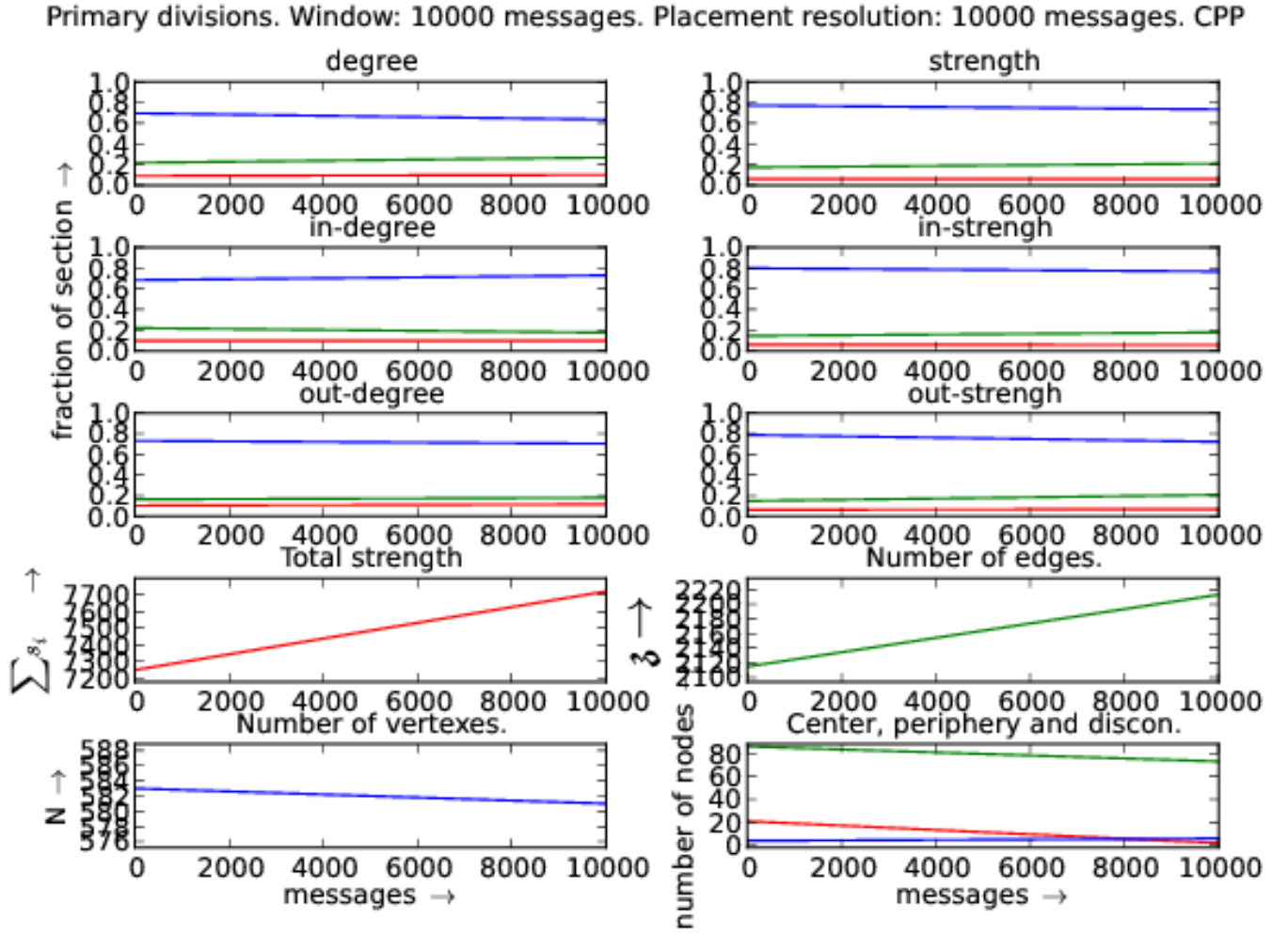


FIG. 6. Distribution of vertices with respect to each centrality measure: in and out degrees and strengths. CPP Std library official mailing list. In the first six plots, red is fraction of hubs, green is the fraction of intermediary and blue is for peripheral fraction. On the last plot, red is the center (maximum distance to another vertex is equal to radius), blue is periphery (maximum distance equals to diameter) of the giant component. On the same graph, green counts the disconnected vertices.

Compound divisions. Window: 10000 messages. Placement resolution: 10000 messages. CPP

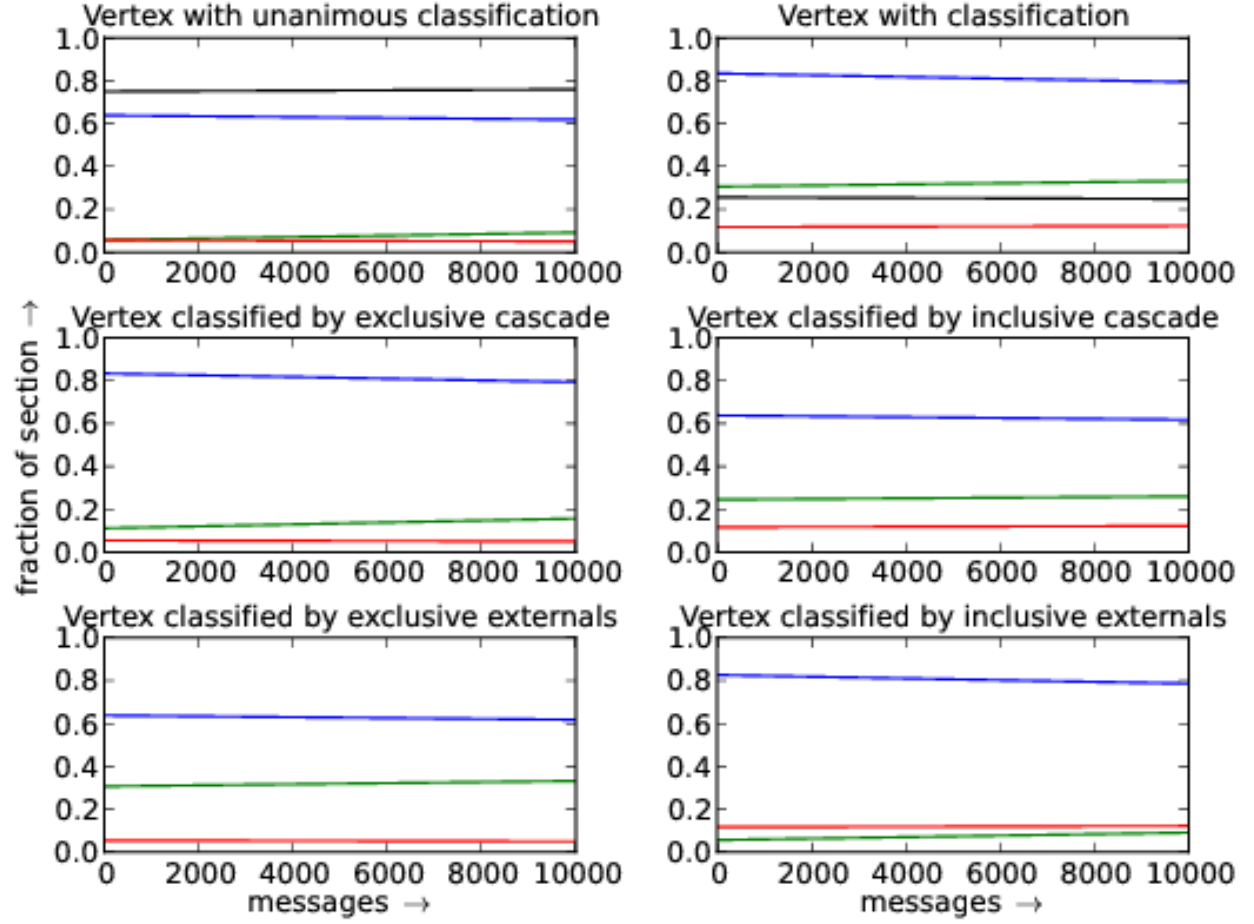


FIG. 7. Distribution of vertex with respect to compound criteria. Red, green and blue designate hubs, intermediary and border (peripheral) vertex fractions. The first two plots exhibit classifications that are not functions. Thus, in the first plot, the fraction of vertices with unique classification is plotted in black. On the second plot, black represents the fraction of vertices that has more than one class: $\frac{\text{number of classifications} - \text{number of nodes}}{\text{number of nodes}}$. Compound criteria is described in Section III B 1.

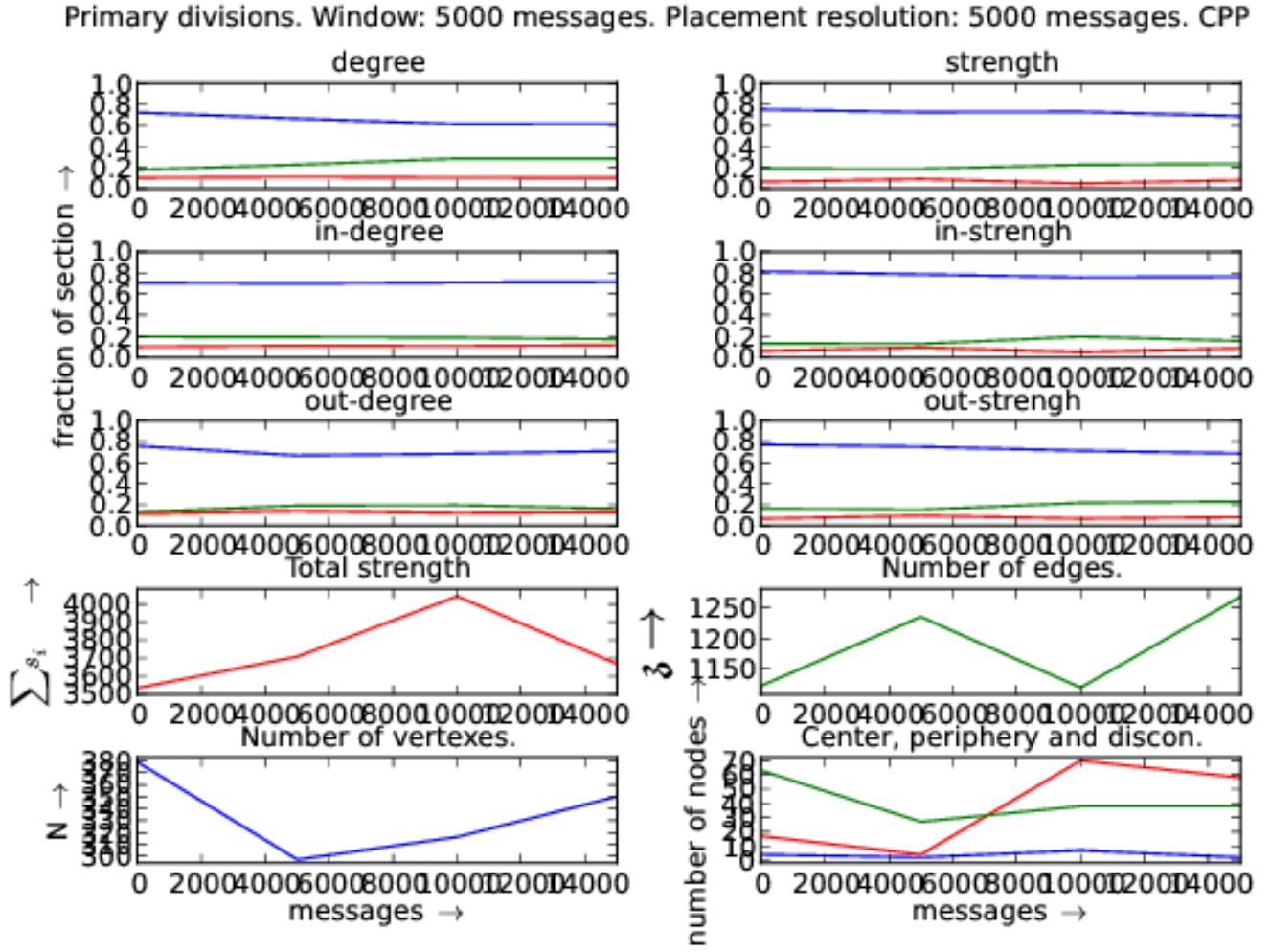


FIG. 8. Distribution of vertices with respect to each centrality measure: in and out degrees and strengths. CPP Std library official mailing list. In the first six plots, red is fraction of hubs, green is the fraction of intermediary and blue is for peripheral fraction. On the last plot, red is the center (maximum distance to another vertex is equal to radius), blue is periphery (maximum distance equals to diameter) of the giant component. On the same graph, green counts the disconnected vertices.

Compound divisions. Window: 5000 messages. Placement resolution: 5000 messages. CPP

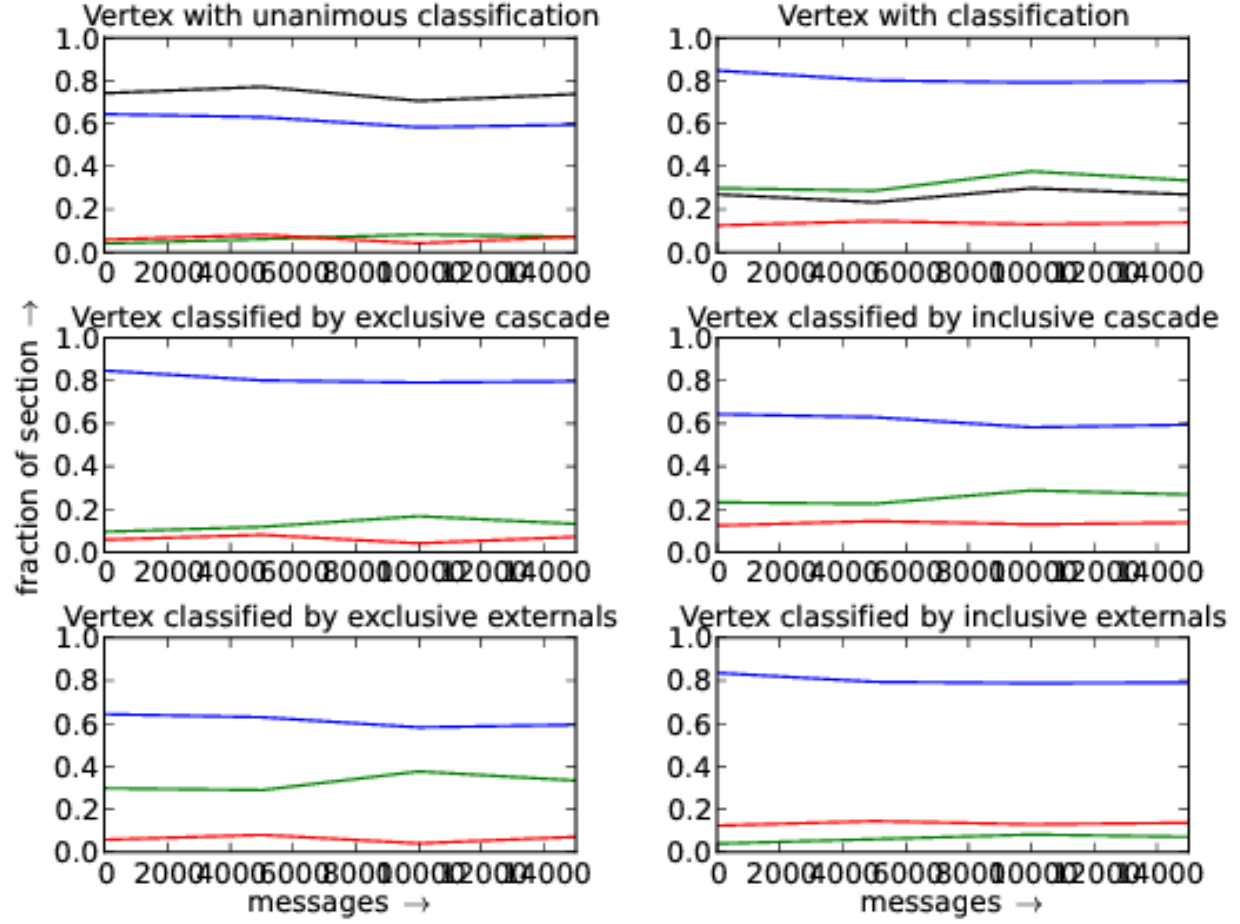


FIG. 9. Distribution of vertex with respect to compound criteria. Red, green and blue designate hubs, intermediary and border (peripheral) vertex fractions. The first two plots exhibit classifications that are not functions. Thus, in the first plot, the fraction of vertices with unique classification is plotted in black. On the second plot, black represents the fraction of vertices that has more than one class: $\frac{\text{number of classifications} - \text{number of nodes}}{\text{number of nodes}}$. Compound criteria is described in Section III B 1.

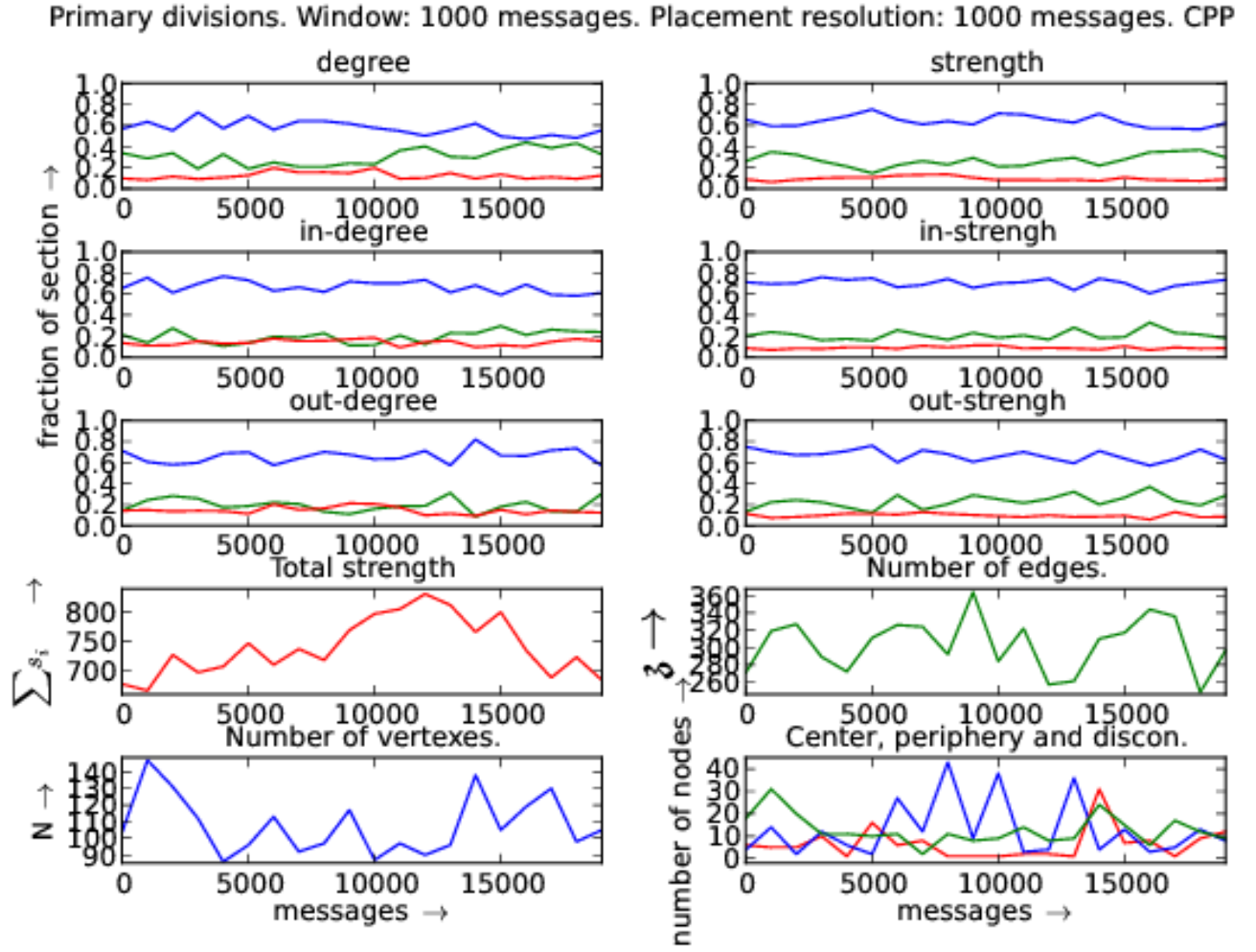


FIG. 10. Distribution of vertices with respect to each centrality measure: in and out degrees and strengths. CPP Std library official mailing list. In the first six plots, red is fraction of hubs, green is the fraction of intermediary and blue is for peripheral fraction. On the last plot, red is the center (maximum distance to another vertex is equal to radius), blue is periphery (maximum distance equals to diameter) of the giant component. On the same graph, green counts the disconnected vertices.

Compound divisions. Window: 1000 messages. Placement resolution: 1000 messages. CPP

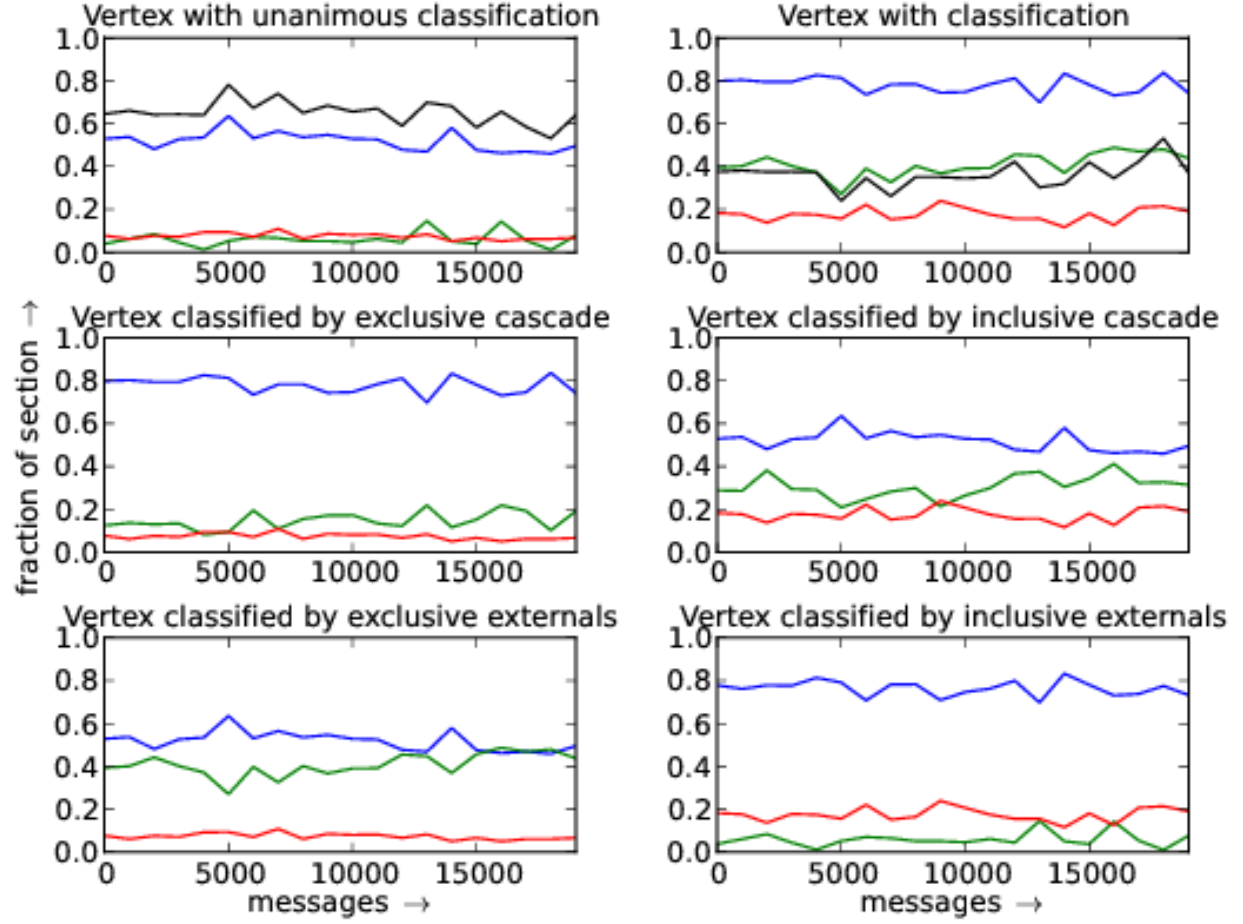


FIG. 11. Distribution of vertex with respect to compound criteria. Red, green and blue designate hubs, intermediary and border (peripheral) vertex fractions. The first two plots exhibit classifications that are not functions. Thus, in the first plot, the fraction of vertices with unique classification is plotted in black. On the second plot, black represents the fraction of vertices that has more than one class: $\frac{\text{number of classifications} - \text{number of nodes}}{\text{number of nodes}}$. Compound criteria is described in Section III B 1.

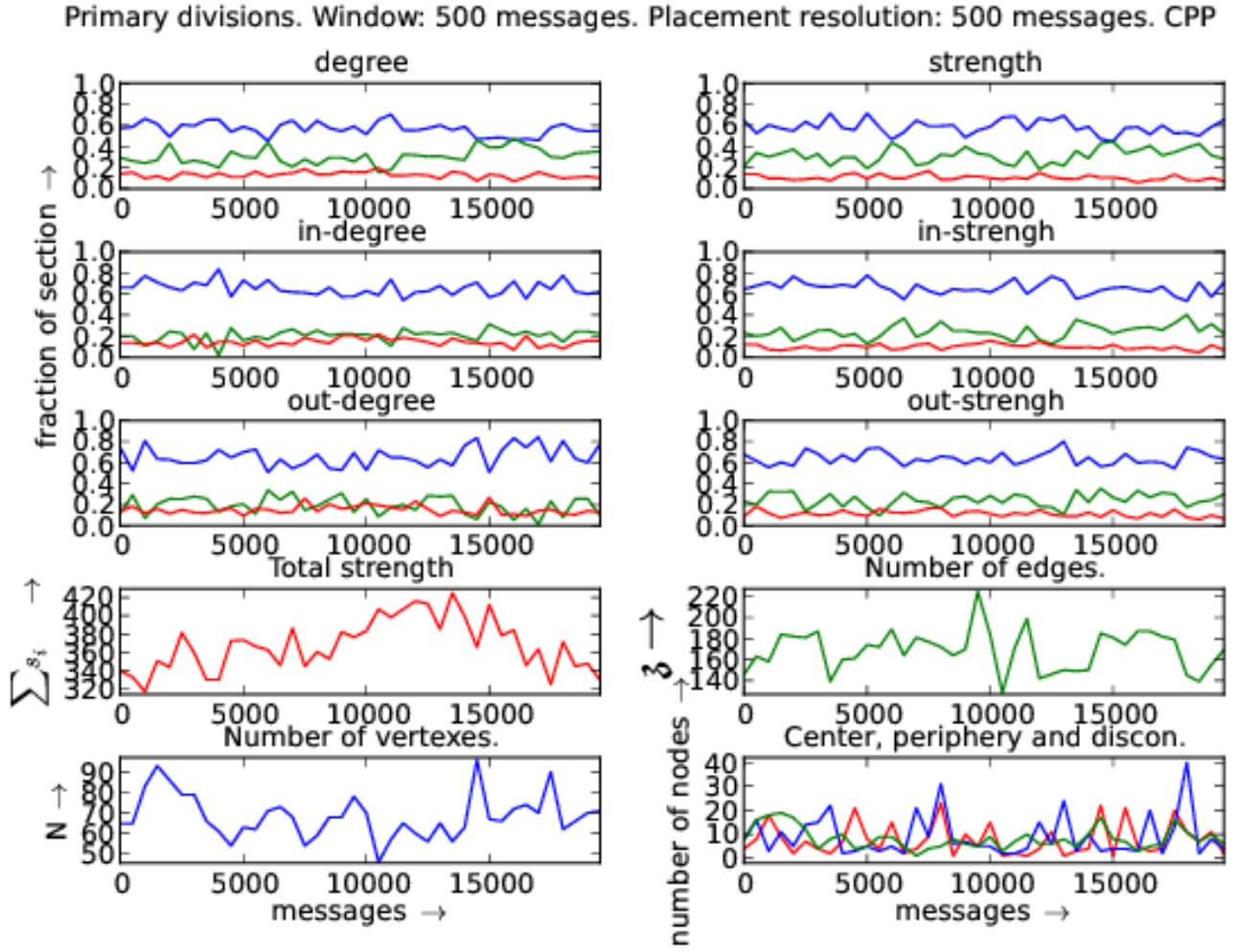


FIG. 12. Distribution of vertices with respect to each centrality measure: in and out degrees and strengths. CPP Std library official mailing list. In the first six plots, red is fraction of hubs, green is the fraction of intermediary and blue is for peripheral fraction. On the last plot, red is the center (maximum distance to another vertex is equal to radius), blue is periphery (maximum distance equals to diameter) of the giant component. On the same graph, green counts the disconnected vertices.

Compound divisions. Window: 500 messages. Placement resolution: 500 messages. CPP

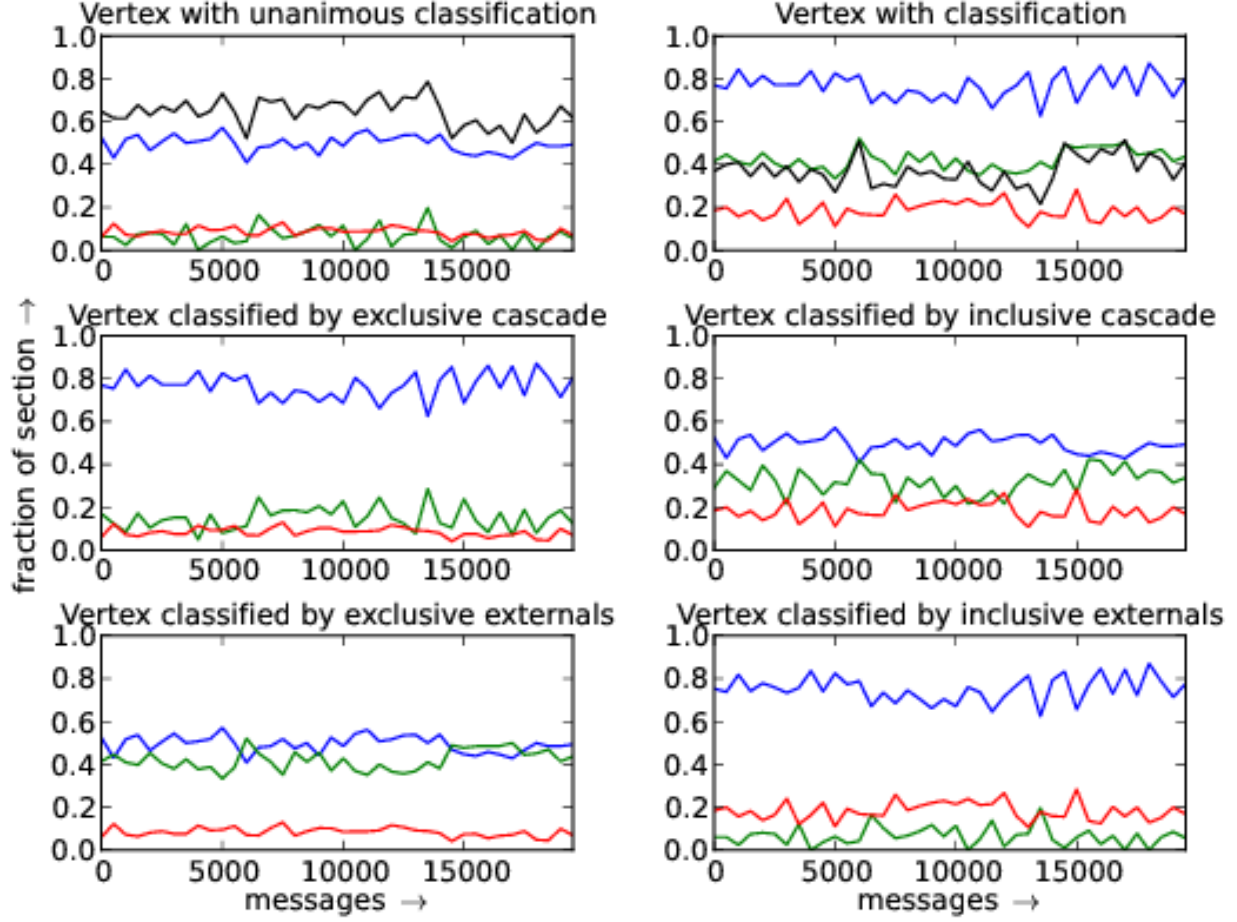


FIG. 13. Distribution of vertex with respect to compound criteria. Red, green and blue designate hubs, intermediary and border (peripheral) vertex fractions. The first two plots exhibit classifications that are not functions. Thus, in the first plot, the fraction of vertices with unique classification is plotted in black. On the second plot, black represents the fraction of vertices that has more than one class: $\frac{\text{number of classifications} - \text{number of nodes}}{\text{number of nodes}}$. Compound criteria is described in Section III B 1.

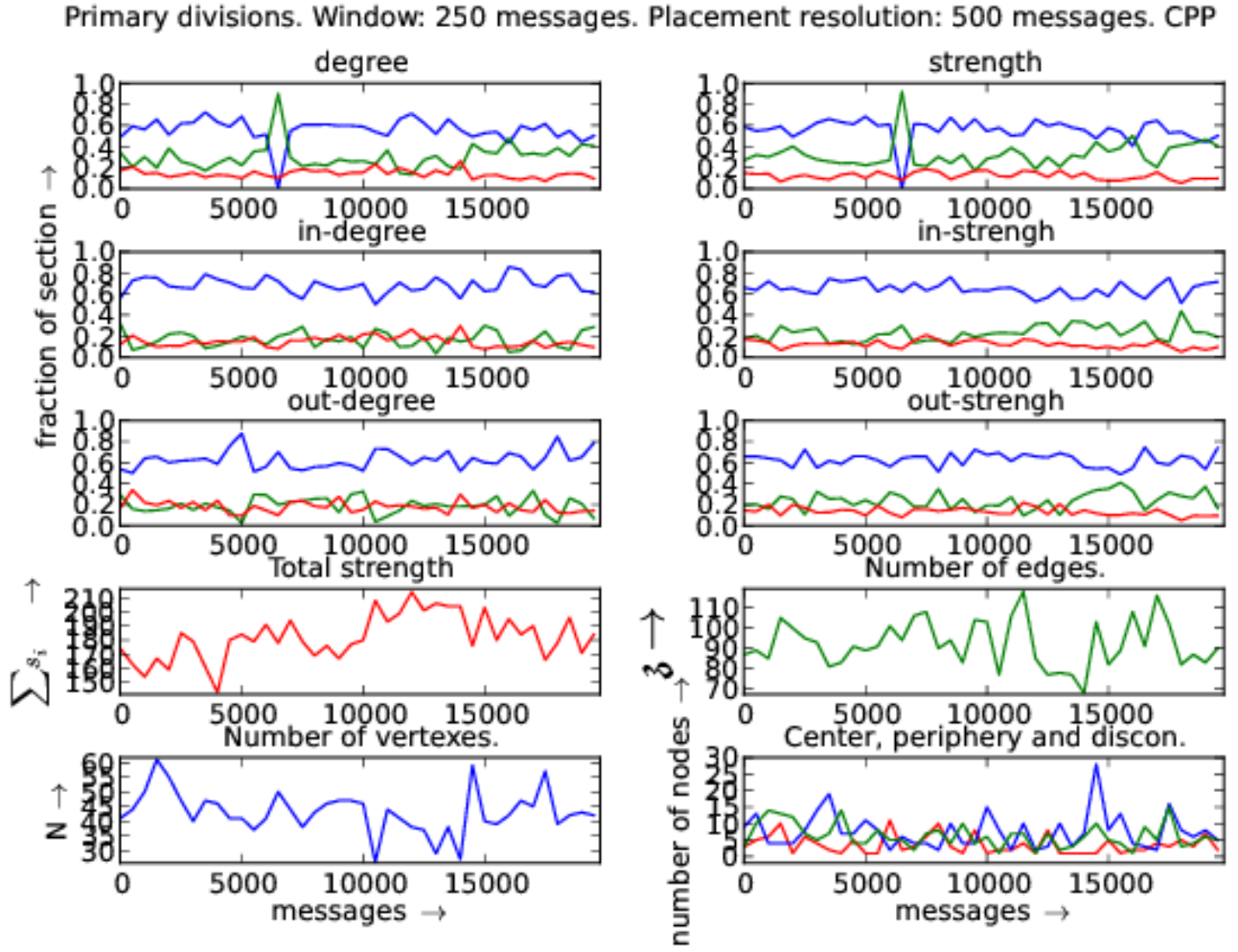


FIG. 14. Distribution of vertices with respect to each centrality measure: in and out degrees and strengths. CPP Std library official mailing list. In the first six plots, red is fraction of hubs, green is the fraction of intermediary and blue is for peripheral fraction. On the last plot, red is the center (maximum distance to another vertex is equal to radius), blue is periphery (maximum distance equals to diameter) of the giant component. On the same graph, green counts the disconnected vertices.

Compound divisions. Window: 250 messages. Placement resolution: 500 messages. CPP

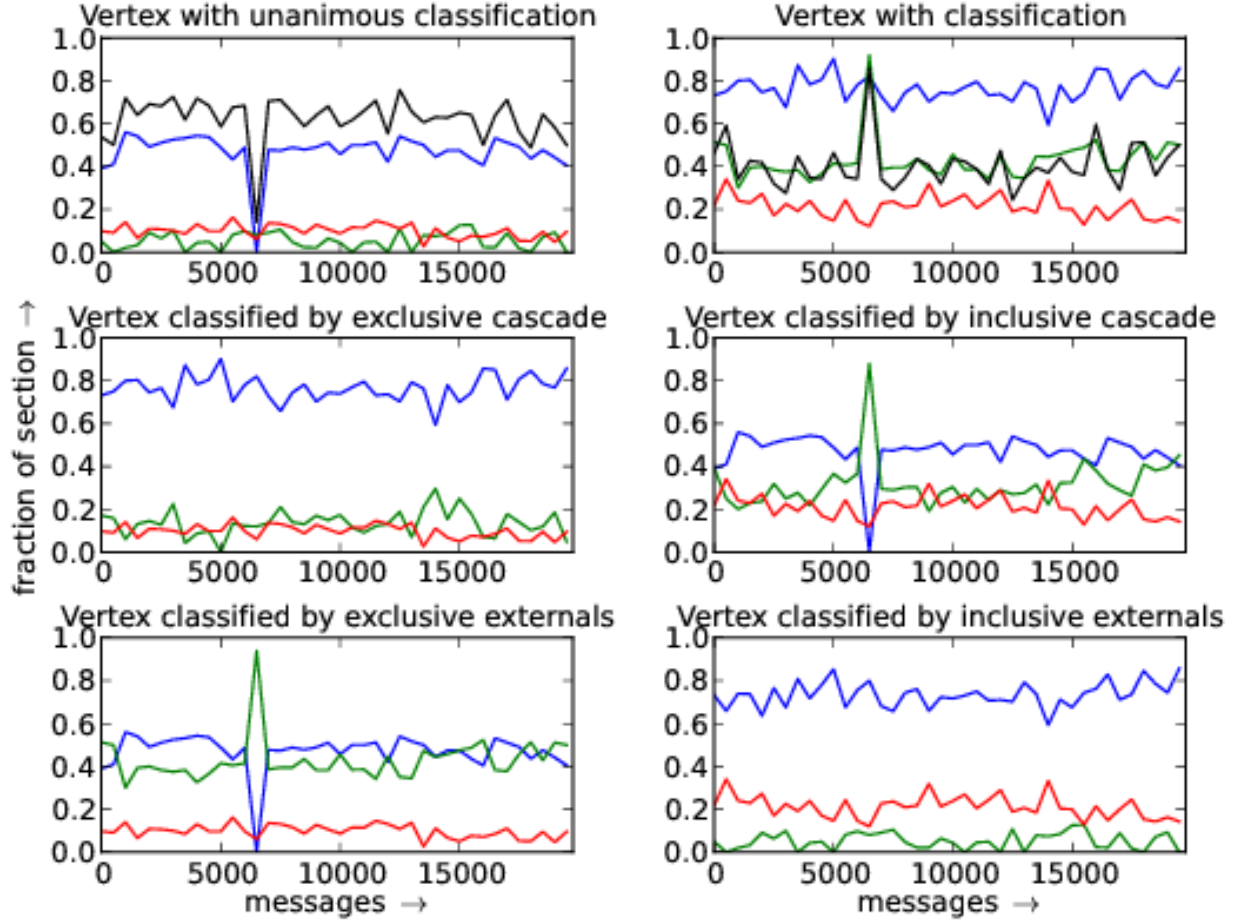


FIG. 15. Distribution of vertex with respect to compound criteria. Red, green and blue designate hubs, intermediary and border (peripheral) vertex fractions. The first two plots exhibit classifications that are not functions. Thus, in the first plot, the fraction of vertices with unique classification is plotted in black. On the second plot, black represents the fraction of vertices that has more than one class: $\frac{\text{number of classifications} - \text{number of nodes}}{\text{number of nodes}}$. Compound criteria is described in Section III B 1.

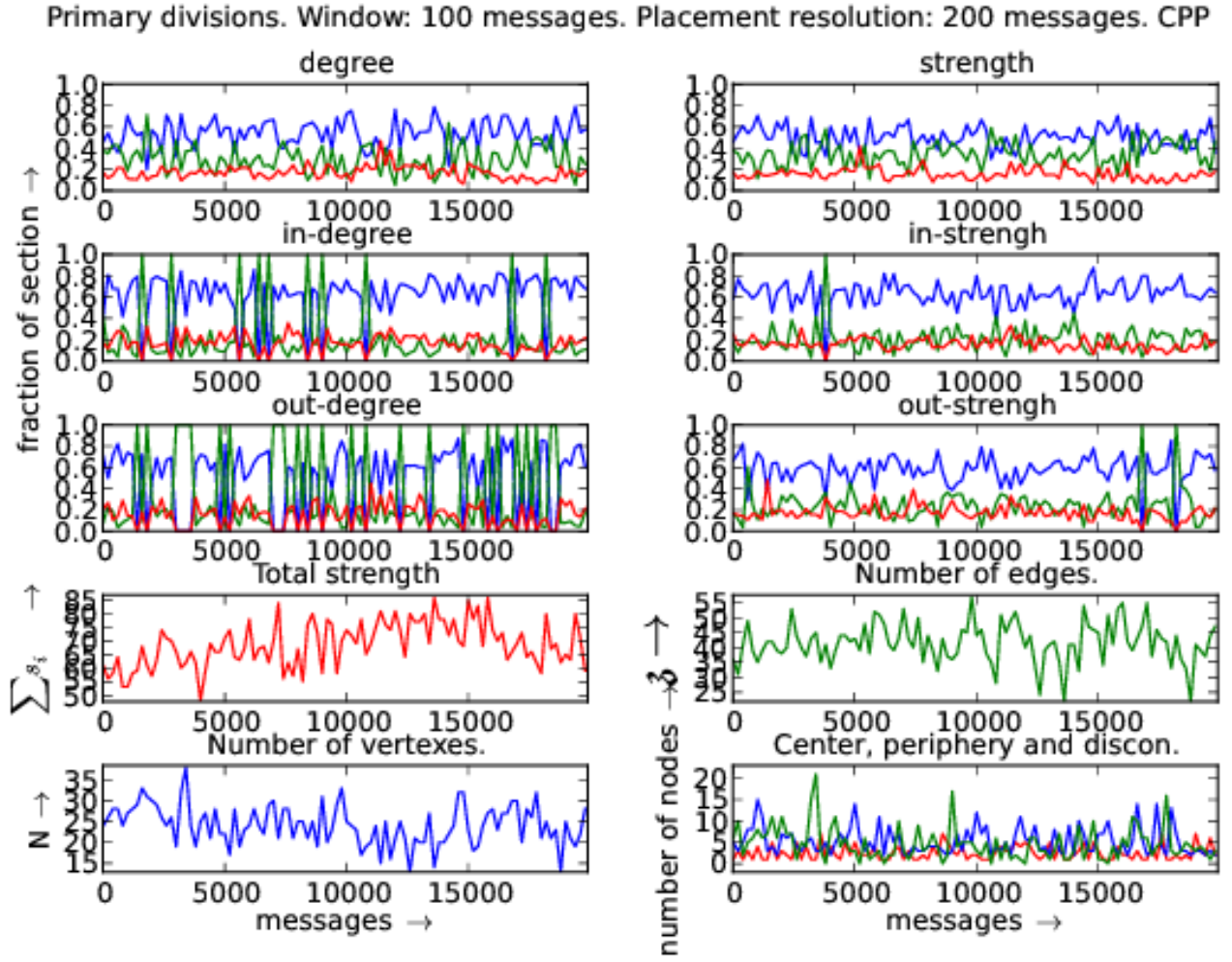


FIG. 16. Distribution of vertices with respect to each centrality measure: in and out degrees and strengths. CPP Std library official mailing list. In the first six plots, red is fraction of hubs, green is the fraction of intermediary and blue is for peripheral fraction. On the last plot, red is the center (maximum distance to another vertex is equal to radius), blue is periphery (maximum distance equals to diameter) of the giant component. On the same graph, green counts the disconnected vertices.

Compound divisions. Window: 100 messages. Placement resolution: 200 messages. CPP

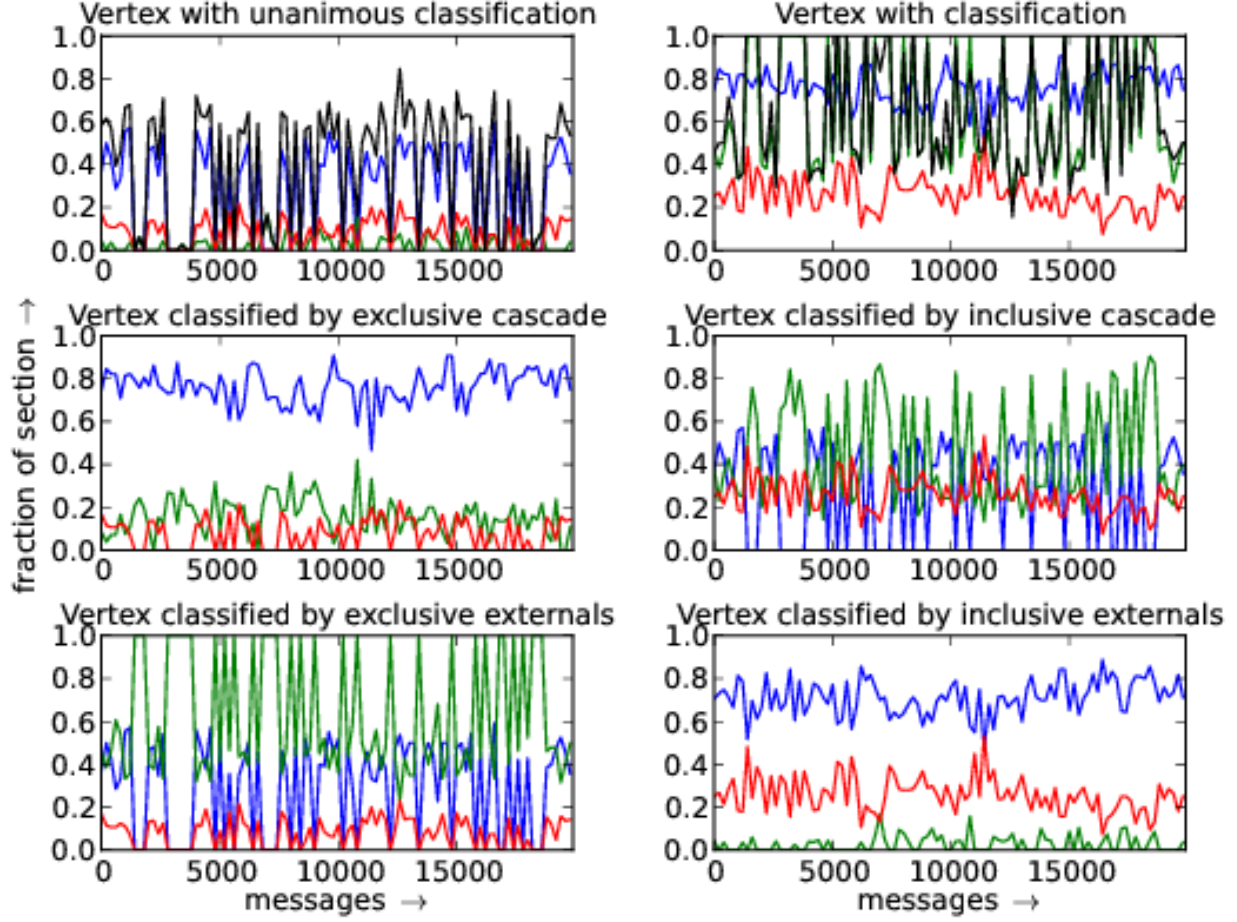


FIG. 17. Distribution of vertex with respect to compound criteria. Red, green and blue designate hubs, intermediary and border (peripheral) vertex fractions. The first two plots exhibit classifications that are not functions. Thus, in the first plot, the fraction of vertices with unique classification is plotted in black. On the second plot, black represents the fraction of vertices that has more than one class: $\frac{\text{number of classifications} - \text{number of nodes}}{\text{number of nodes}}$. Compound criteria is described in Section III B 1.

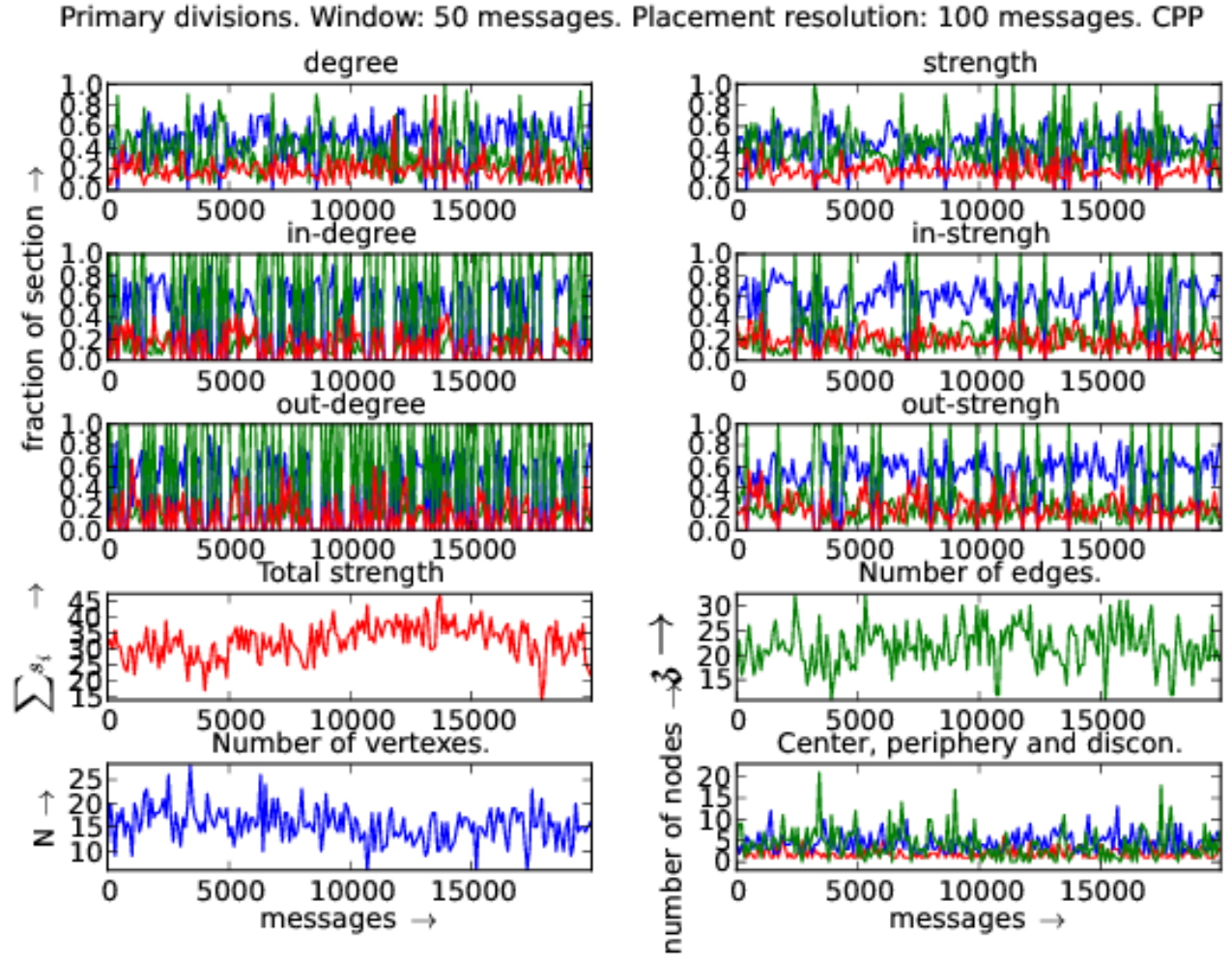


FIG. 18. Distribution of vertices with respect to each centrality measure: in and out degrees and strengths. CPP Std library official mailing list. In the first six plots, red is fraction of hubs, green is the fraction of intermediary and blue is for peripheral fraction. On the last plot, red is the center (maximum distance to another vertex is equal to radius), blue is periphery (maximum distance equals to diameter) of the giant component. On the same graph, green counts the disconnected vertices.

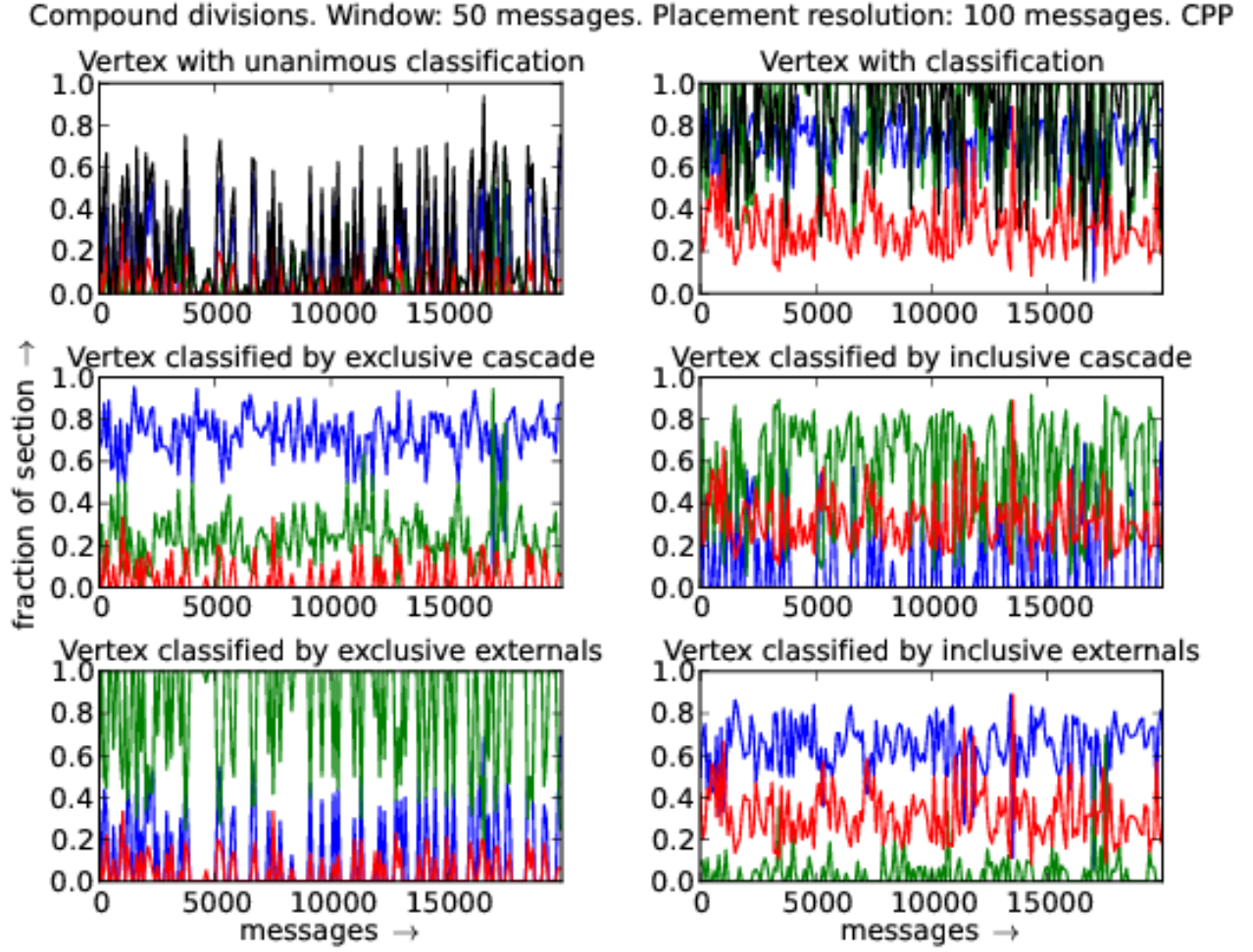


FIG. 19. Distribution of vertex with respect to compound criteria. Red, green and blue designate hubs, intermediary and border (peripheral) vertex fractions. The first two plots exhibit classifications that are not functions. Thus, in the first plot, the fraction of vertices with unique classification is plotted in black. On the second plot, black represents the fraction of vertices that has more than one class: $\frac{\text{number of classifications} - \text{number of nodes}}{\text{number of nodes}}$. Compound criteria is described in Section III B 1.

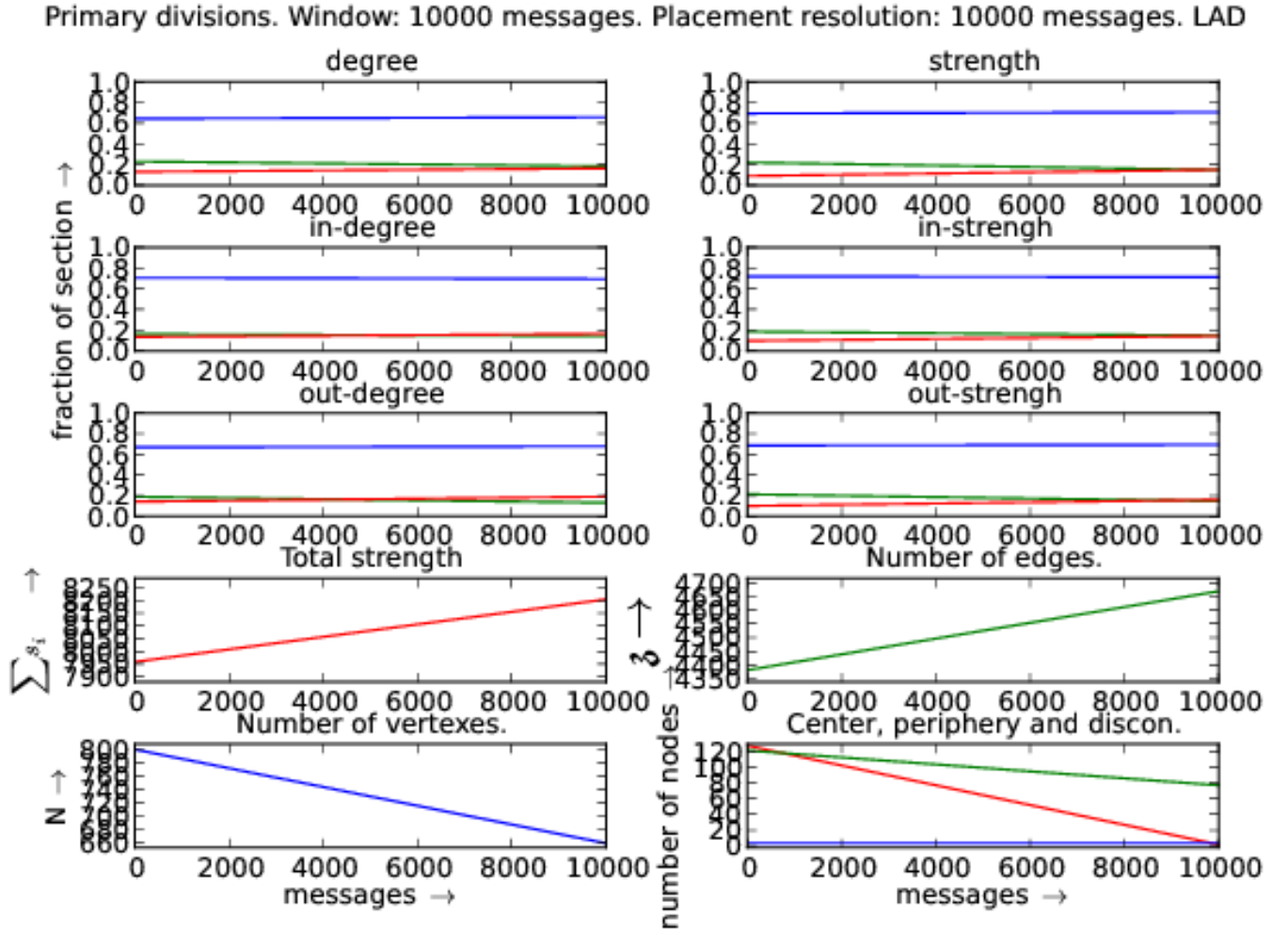


FIG. 20. Distribution of vertices with respect to each centrality measure: in and out degrees and strengths. Linux Audio Users (LAD) official mailing list. In the first six plots, red is fraction of hubs, green is the fraction of intermediary and blue is for peripheral fraction. On the last plot, red is the center (maximum distance to another vertex is equal to radius), blue is periphery (maximum distance equals to diameter) of the giant component. On the same graph, green counts the disconnected vertices.

Compound divisions. Window: 10000 messages. Placement resolution: 10000 messages. LAD

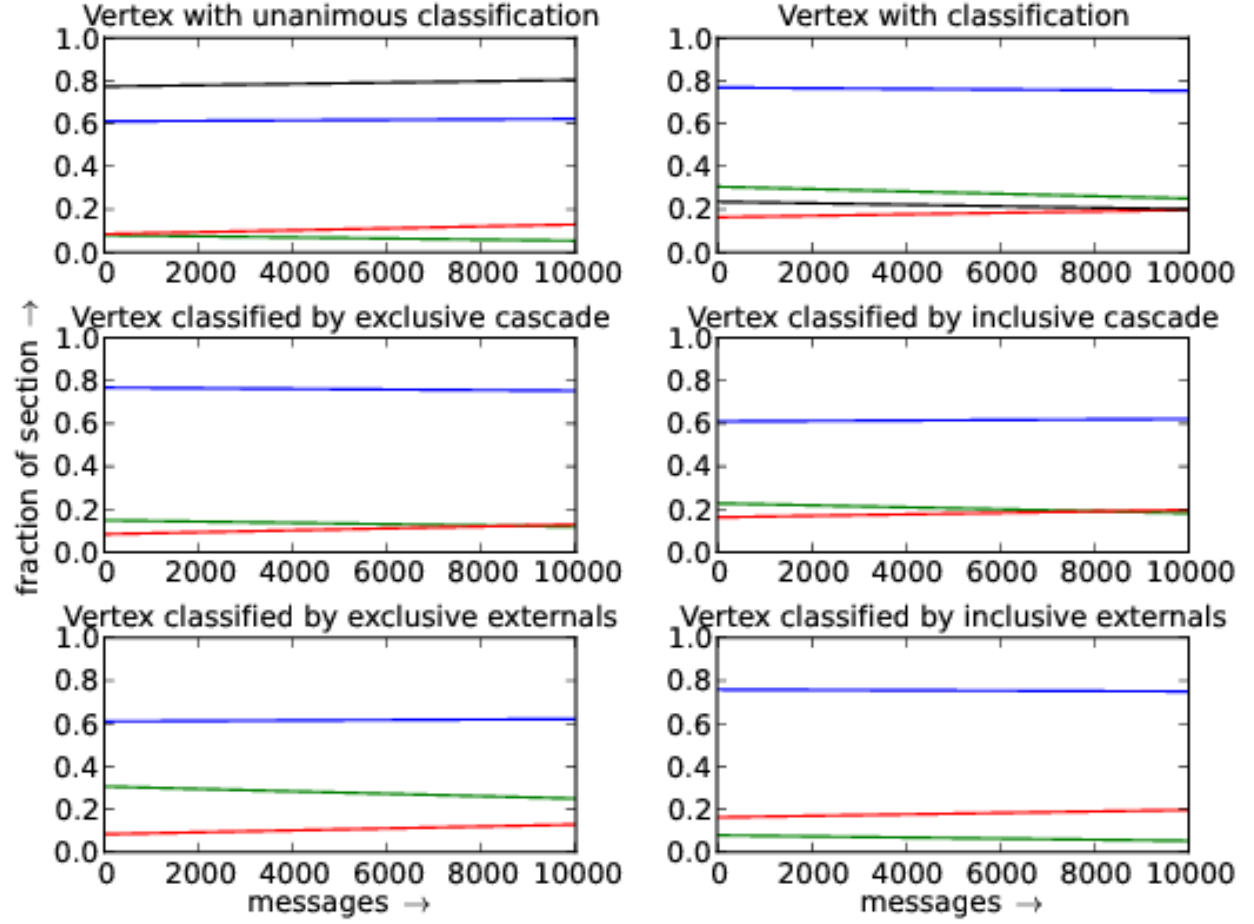


FIG. 21. Distribution of vertex with respect to compound criteria. Red, green and blue designate hubs, intermediary and border (peripheral) vertex fractions. The first two plots exhibit classifications that are not functions. Thus, in the first plot, the fraction of vertices with unique classification is plotted in black. On the second plot, black represents the fraction of vertices that has more than one class: $\frac{\text{number of classifications} - \text{number of nodes}}{\text{number of nodes}}$. Compound criteria is described in Section III B 1.

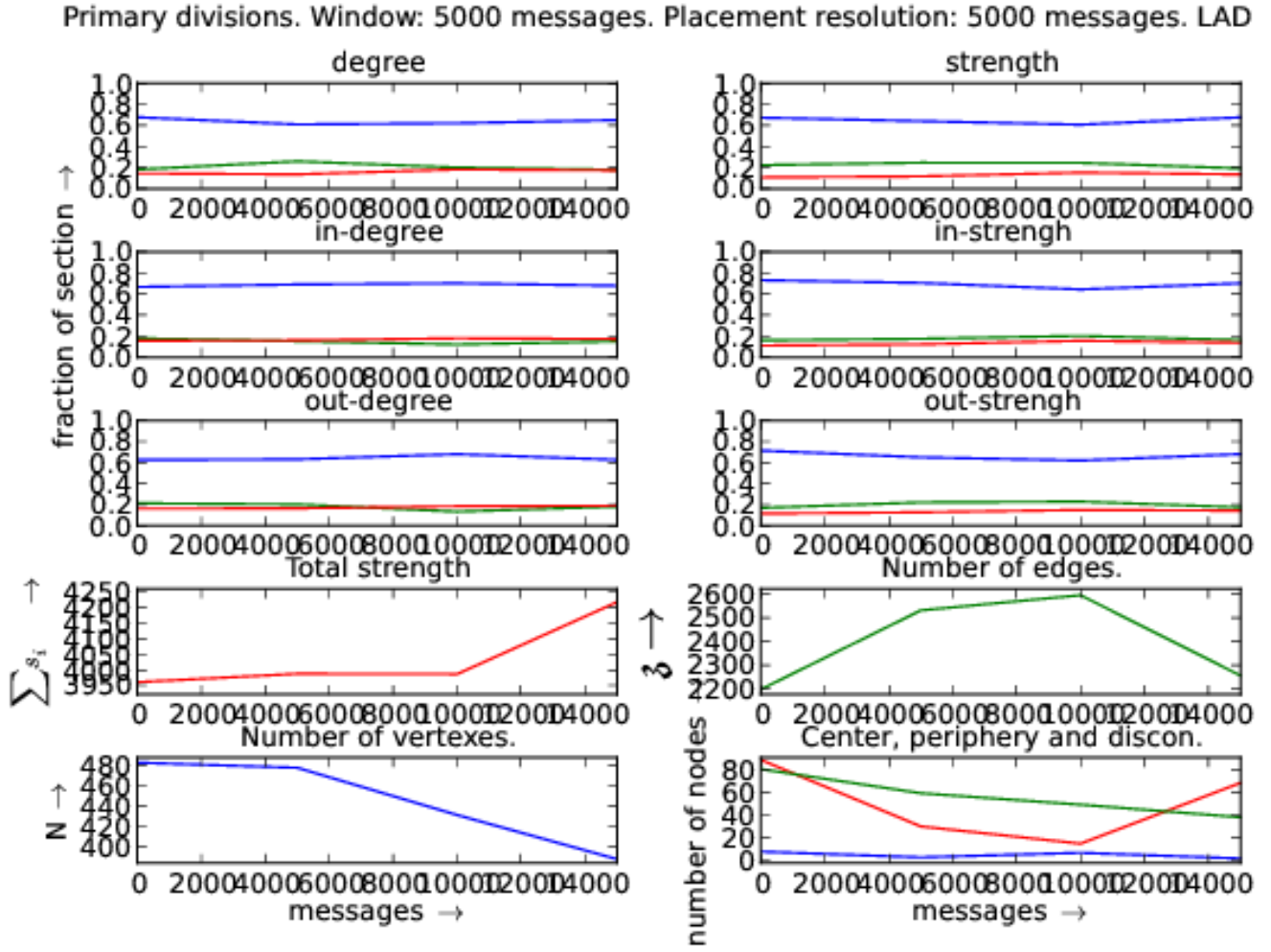


FIG. 22. Distribution of vertices with respect to each centrality measure: in and out degrees and strengths. Linux Audio Users (LAD) official mailing list. In the first six plots, red is fraction of hubs, green is the fraction of intermediary and blue is for periphery fraction. On the last plot, red is the center (maximum distance to another vertex is equal to radius), blue is periphery (maximum distance equals to diameter) of the giant component. On the same graph, green counts the disconnected vertices.

Compound divisions. Window: 5000 messages. Placement resolution: 5000 messages. LAD

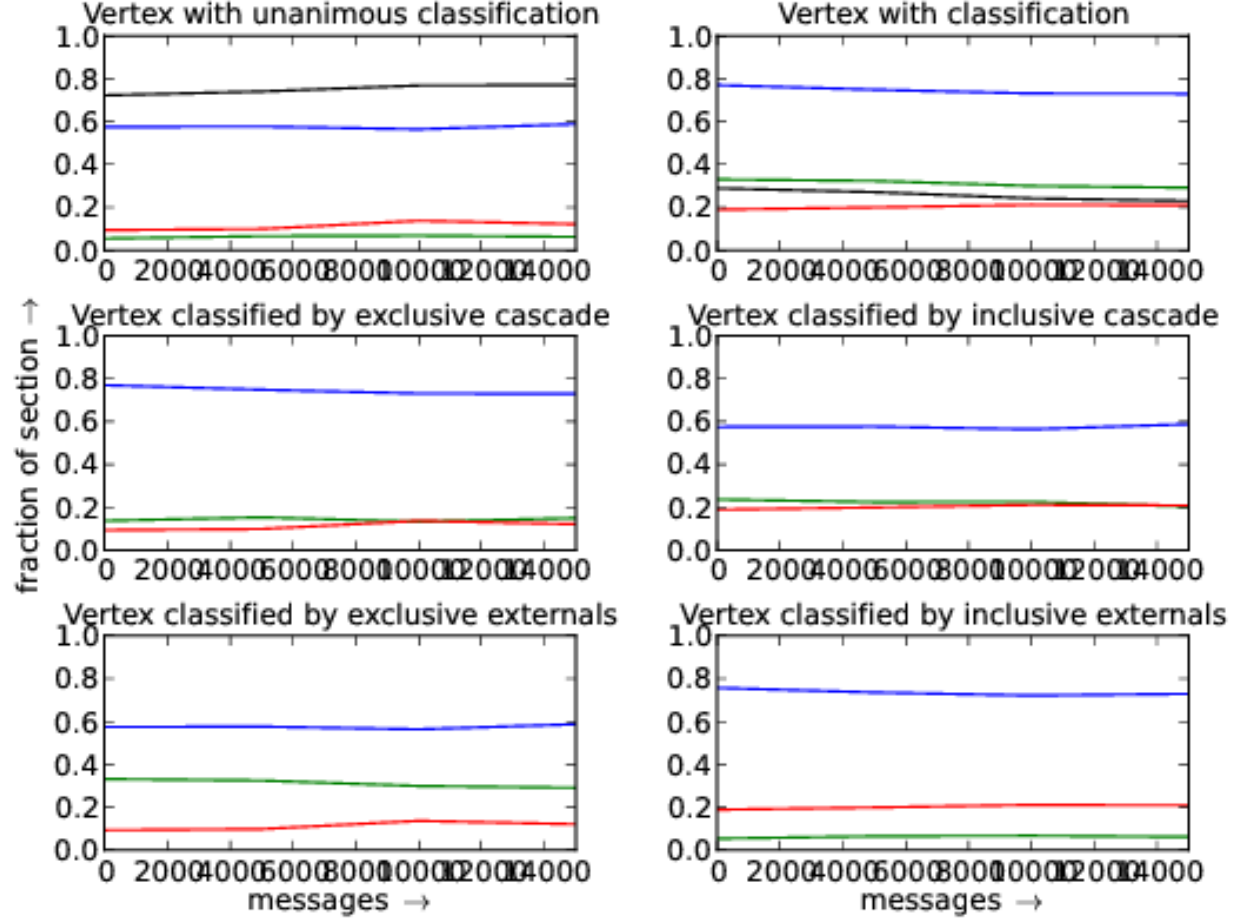


FIG. 23. Distribution of vertex with respect to compound criteria. Red, green and blue designate hubs, intermediary and border (peripheral) vertex fractions. The first two plots exhibit classifications that are not functions. Thus, in the first plot, the fraction of vertices with unique classification is plotted in black. On the second plot, black represents the fraction of vertices that has more than one class: $\frac{\text{number of classifications} - \text{number of nodes}}{\text{number of nodes}}$. Compound criteria is described in Section III B 1.

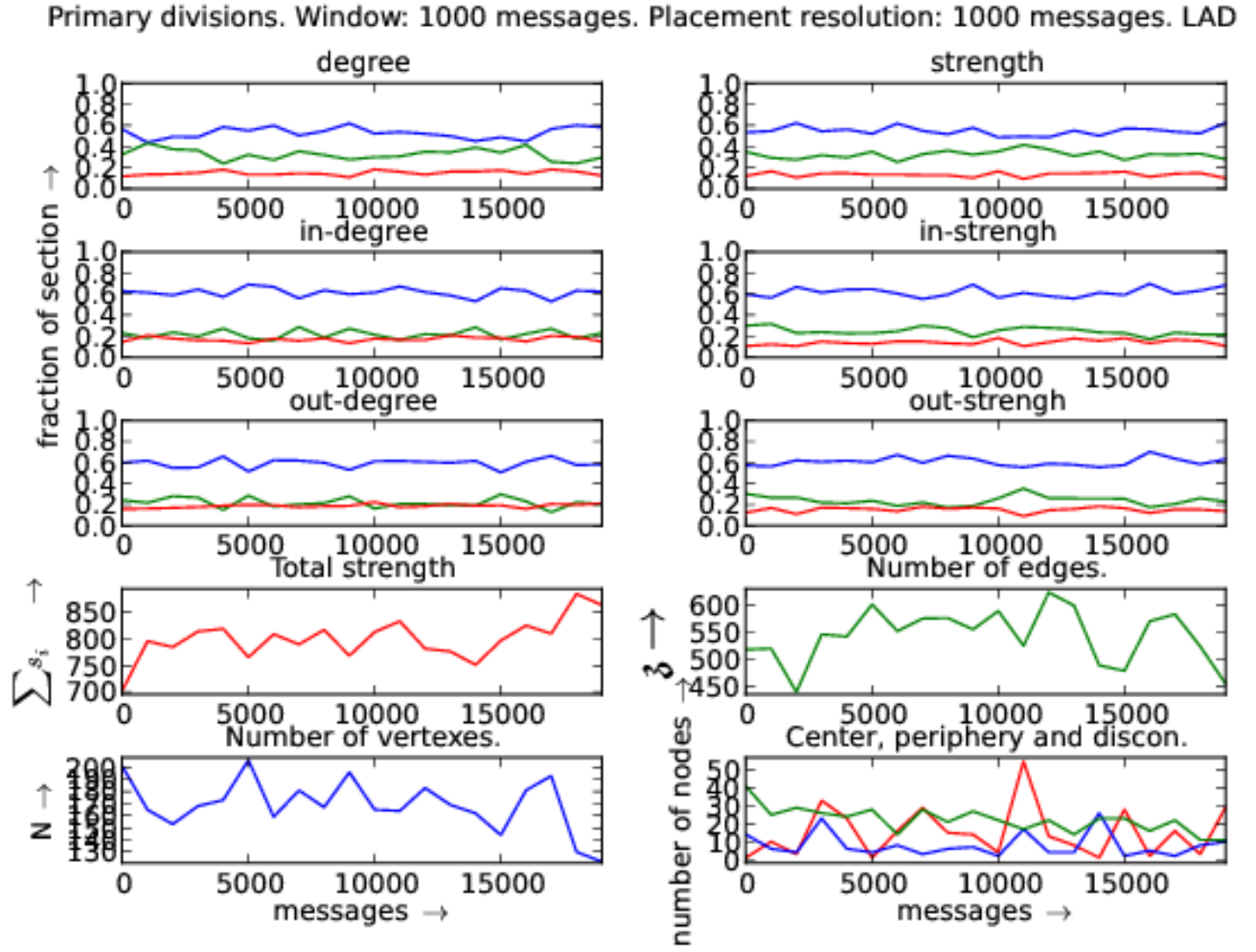


FIG. 24. Distribution of vertices with respect to each centrality measure: in and out degrees and strengths. Linux Audio Users (LAD) official mailing list. In the first six plots, red is fraction of hubs, green is the fraction of intermediary and blue is for peripheral fraction. On the last plot, red is the center (maximum distance to another vertex is equal to radius), blue is periphery (maximum distance equals to diameter) of the giant component. On the same graph, green counts the disconnected vertices.

Compound divisions. Window: 1000 messages. Placement resolution: 1000 messages. LAD

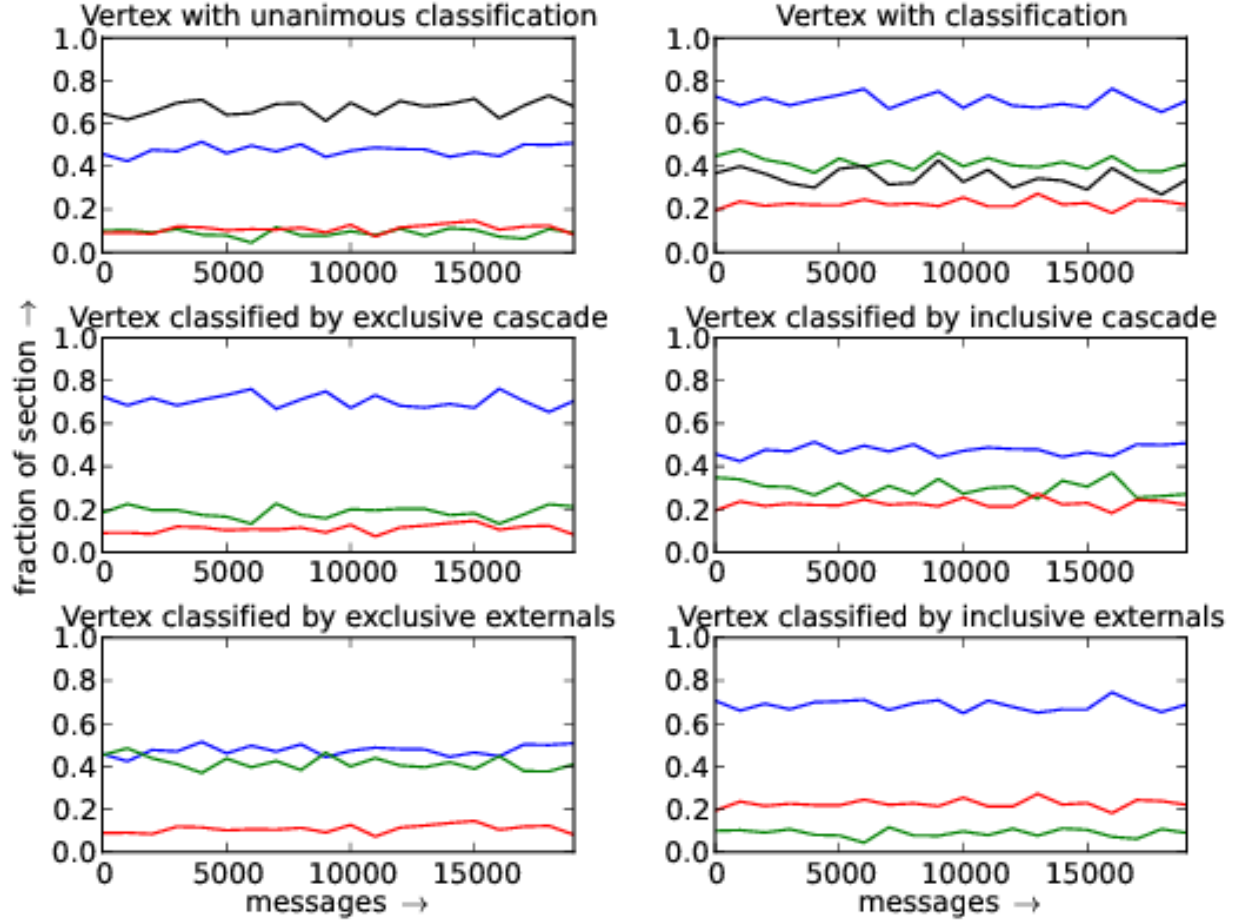


FIG. 25. Distribution of vertex with respect to compound criteria. Red, green and blue designate hubs, intermediary and border (peripheral) vertex fractions. The first two plots exhibit classifications that are not functions. Thus, in the first plot, the fraction of vertices with unique classification is plotted in black. On the second plot, black represents the fraction of vertices that has more than one class: $\frac{\text{number of classifications} - \text{number of nodes}}{\text{number of nodes}}$. Compound criteria is described in Section III B 1.

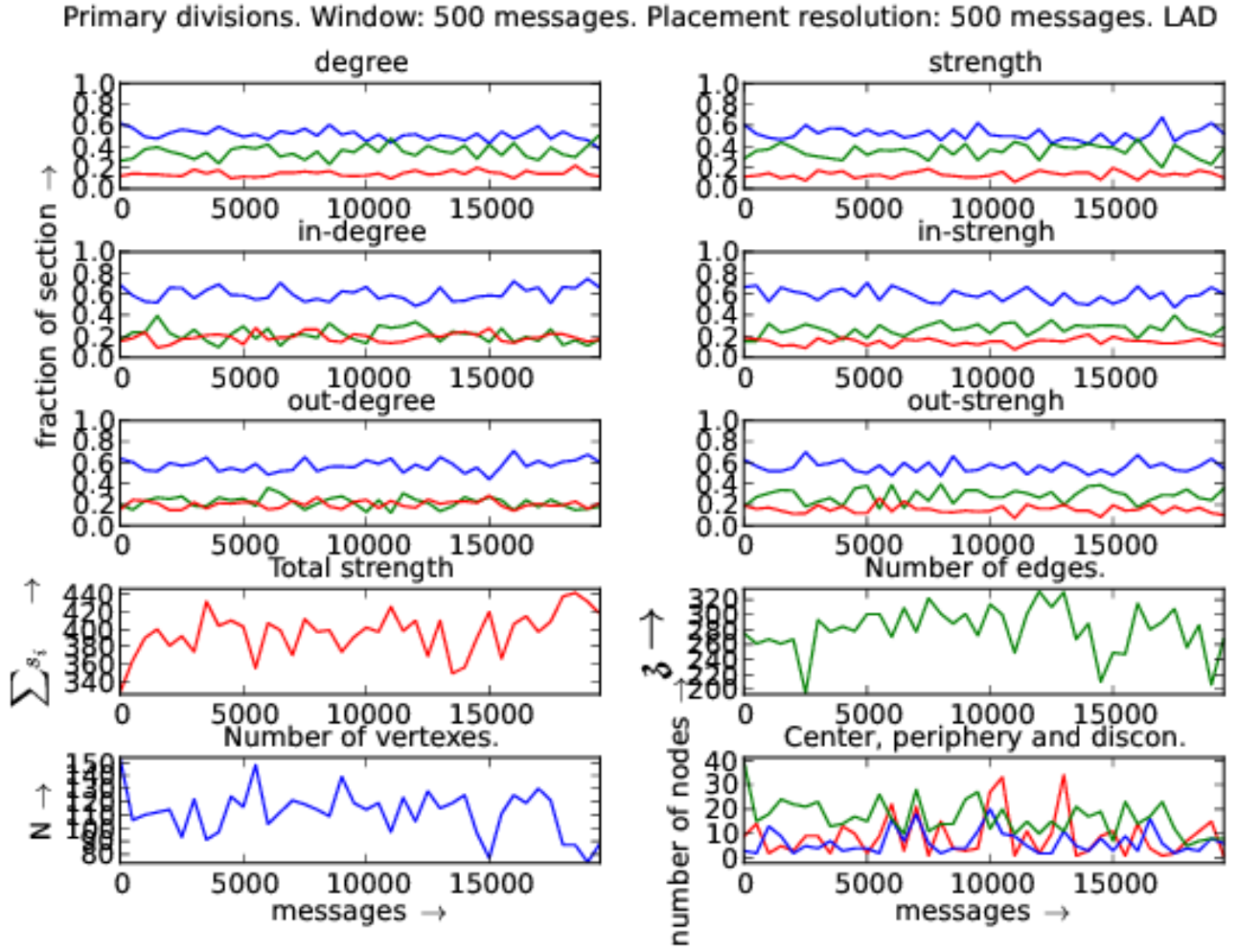


FIG. 26. Distribution of vertices with respect to each centrality measure: in and out degrees and strengths. Linux Audio Users (LAD) official mailing list. In the first six plots, red is fraction of hubs, green is the fraction of intermediary and blue is for peripheral fraction. On the last plot, red is the center (maximum distance to another vertex is equal to radius), blue is periphery (maximum distance equals to diameter) of the giant component. On the same graph, green counts the disconnected vertices.

Compound divisions. Window: 500 messages. Placement resolution: 500 messages. LAD

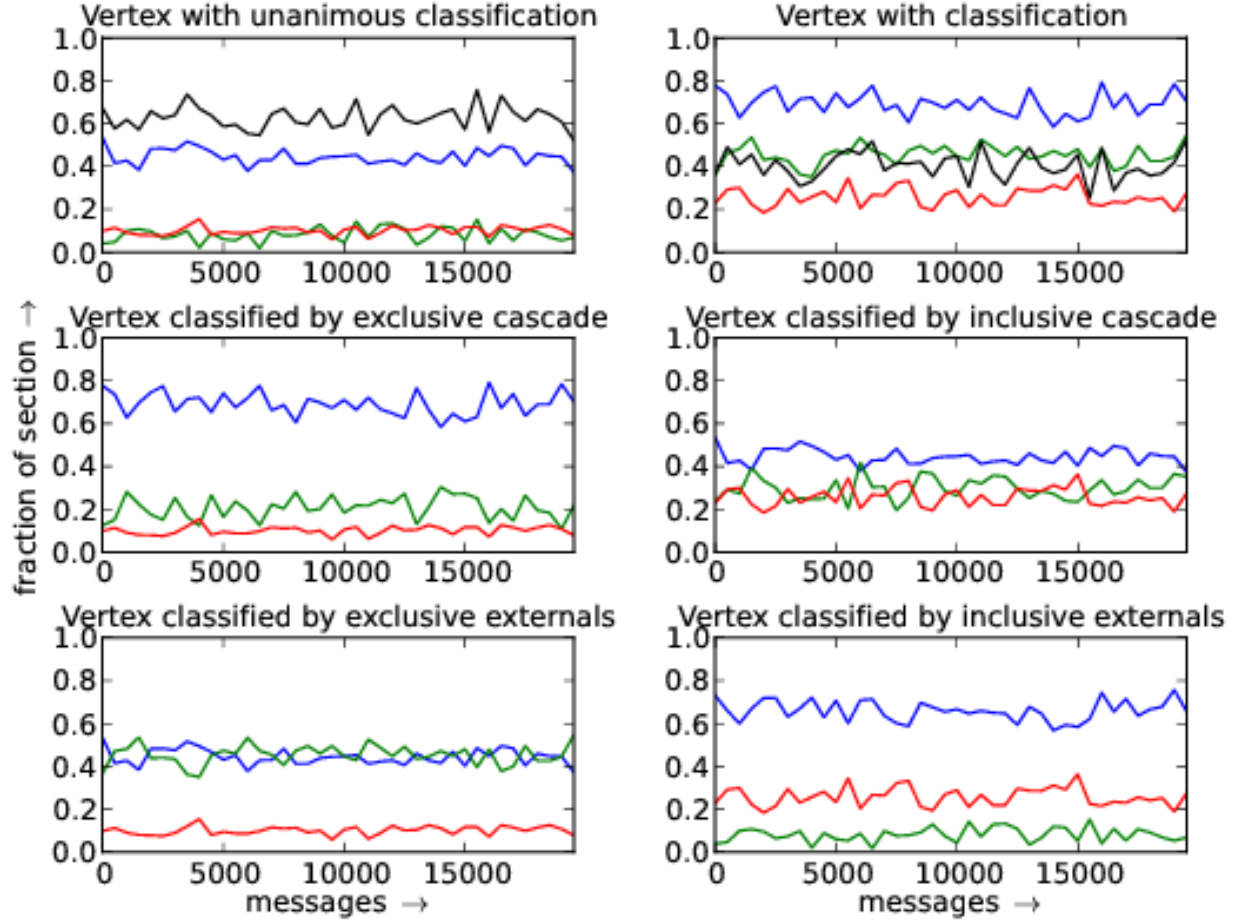


FIG. 27. Distribution of vertex with respect to compound criteria. Red, green and blue designate hubs, intermediary and border (peripheral) vertex fractions. The first two plots exhibit classifications that are not functions. Thus, in the first plot, the fraction of vertices with unique classification is plotted in black. On the second plot, black represents the fraction of vertices that has more than one class: $\frac{\text{number of classifications} - \text{number of nodes}}{\text{number of nodes}}$. Compound criteria is described in Section III B 1.

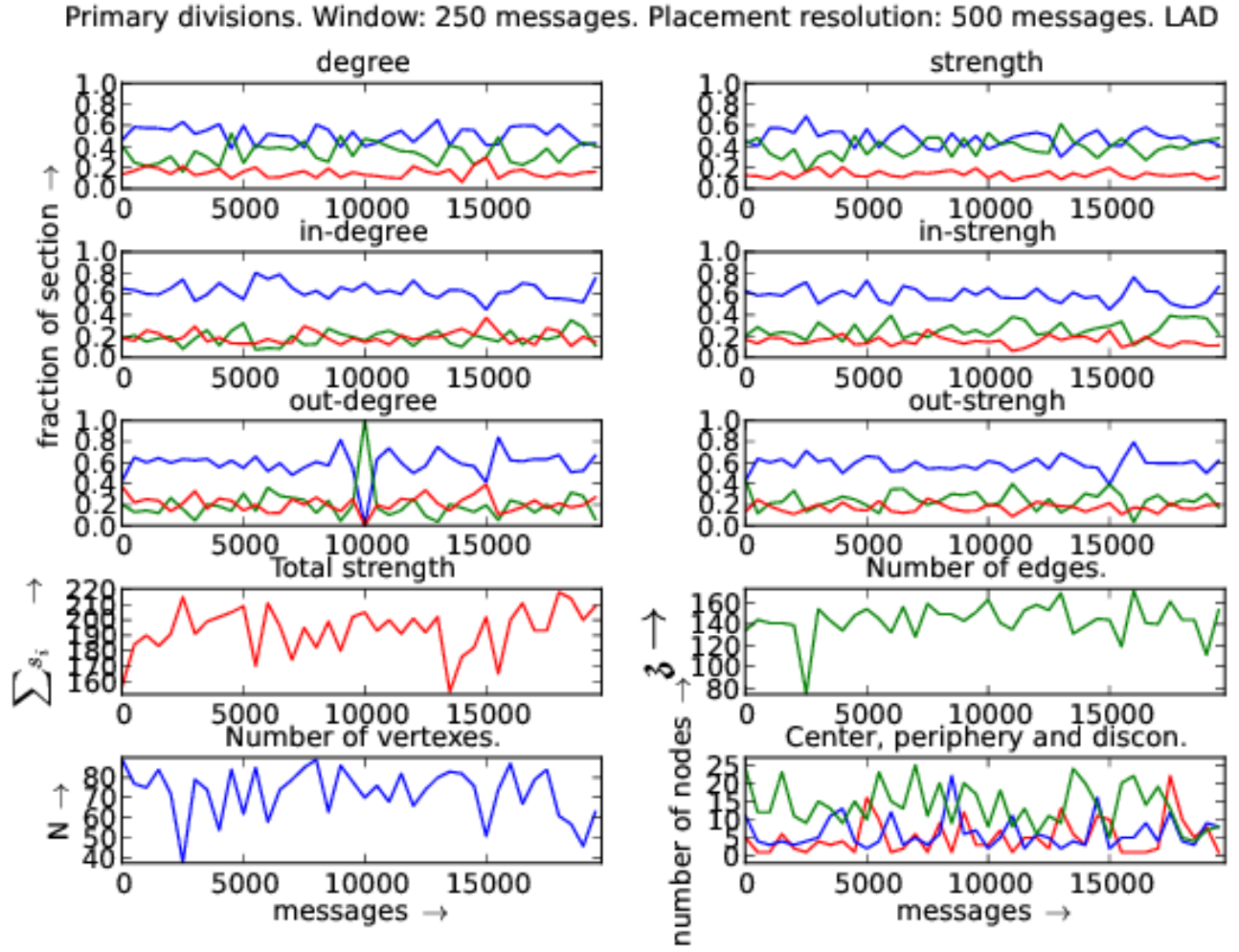


FIG. 28. Distribution of vertices with respect to each centrality measure: in and out degrees and strengths. Linux Audio Users (LAD) official mailing list. In the first six plots, red is fraction of hubs, green is the fraction of intermediary and blue is for peripheral fraction. On the last plot, red is the center (maximum distance to another vertex is equal to radius), blue is periphery (maximum distance equals to diameter) of the giant component. On the same graph, green counts the disconnected vertices.

Compound divisions. Window: 250 messages. Placement resolution: 500 messages. LAD

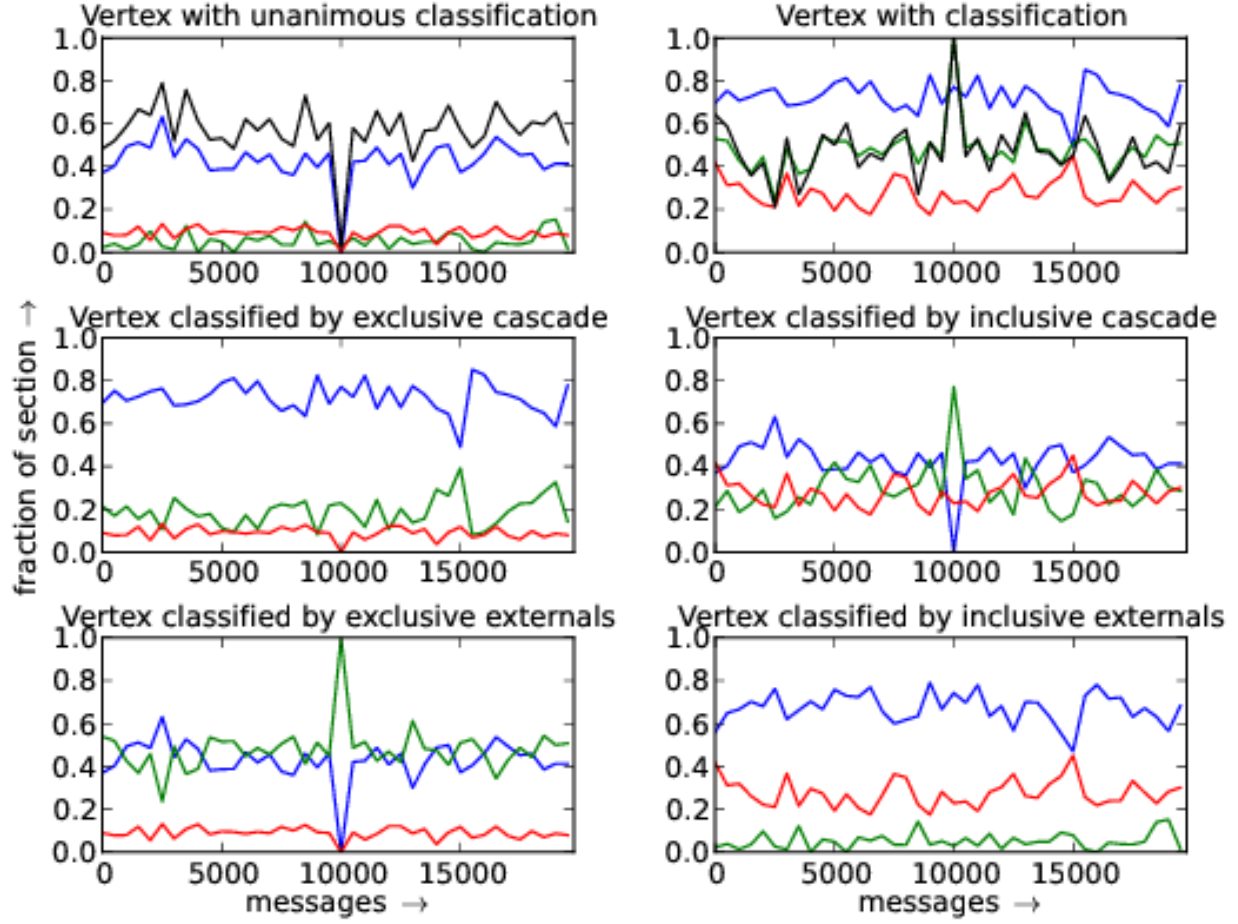


FIG. 29. Distribution of vertex with respect to compound criteria. Red, green and blue designate hubs, intermediary and border (peripheral) vertex fractions. The first two plots exhibit classifications that are not functions. Thus, in the first plot, the fraction of vertices with unique classification is plotted in black. On the second plot, black represents the fraction of vertices that has more than one class: $\frac{\text{number of classifications} - \text{number of nodes}}{\text{number of nodes}}$. Compound criteria is described in Section III B 1.

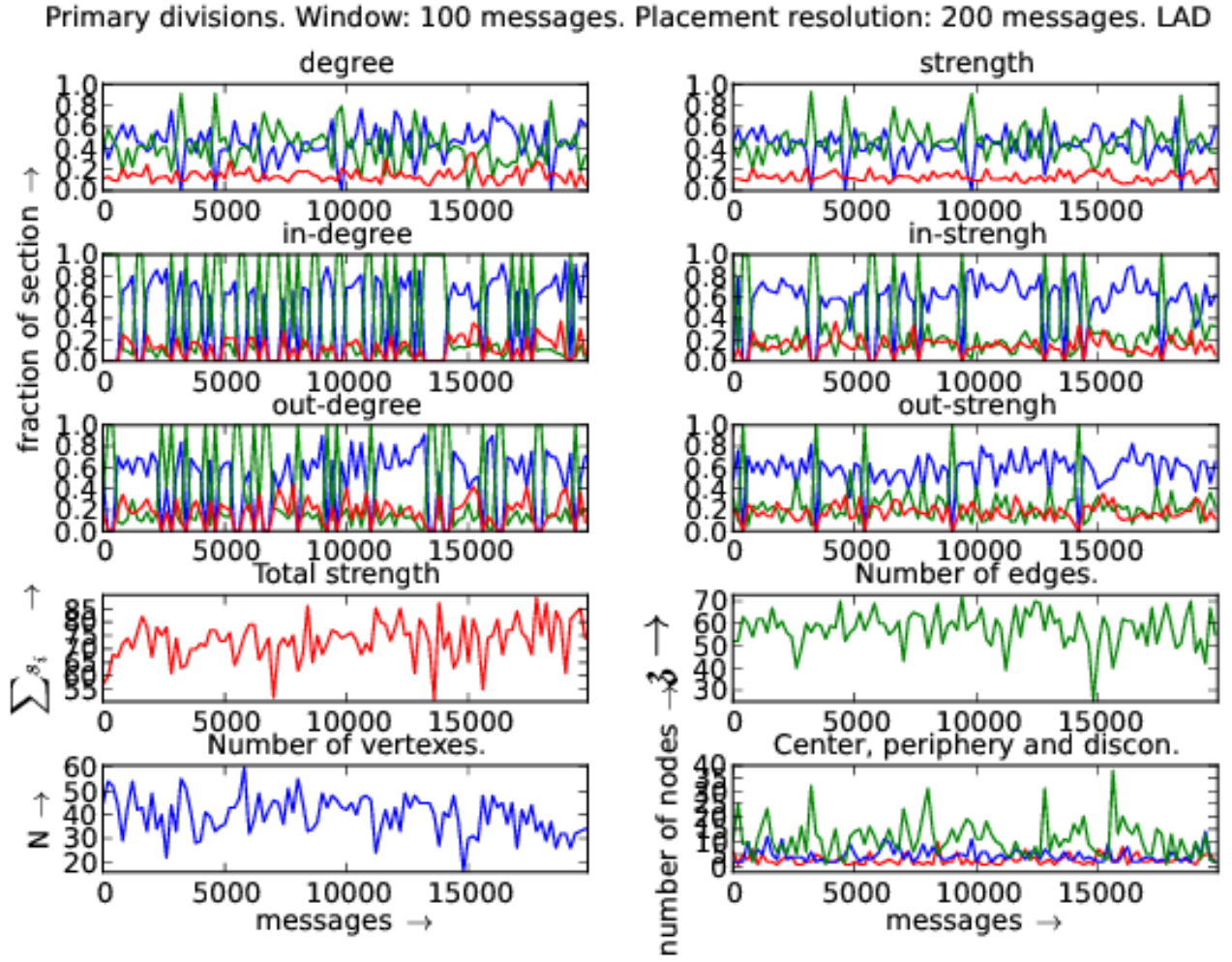


FIG. 30. Distribution of vertices with respect to each centrality measure: in and out degrees and strengths. Linux Audio Users (LAD) official mailing list. In the first six plots, red is fraction of hubs, green is the fraction of intermediary and blue is for peripheral fraction. On the last plot, red is the center (maximum distance to another vertex is equal to radius), blue is periphery (maximum distance equals to diameter) of the giant component. On the same graph, green counts the disconnected vertices.

Compound divisions. Window: 100 messages. Placement resolution: 200 messages. LAD

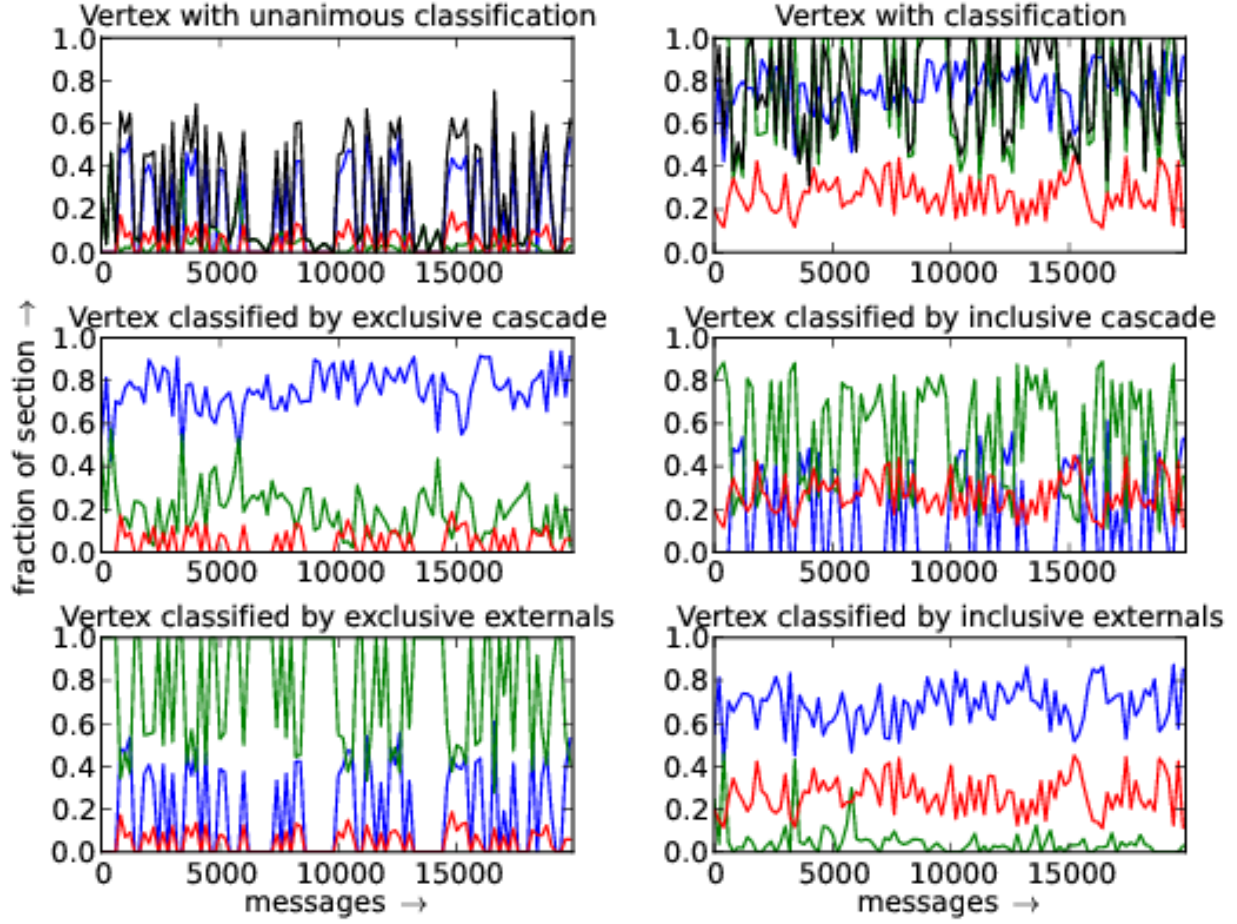


FIG. 31. Distribution of vertex with respect to compound criteria. Red, green and blue designate hubs, intermediary and border (peripheral) vertex fractions. The first two plots exhibit classifications that are not functions. Thus, in the first plot, the fraction of vertices with unique classification is plotted in black. On the second plot, black represents the fraction of vertices that has more than one class: $\frac{\text{number of classifications} - \text{number of nodes}}{\text{number of nodes}}$. Compound criteria is described in Section III B 1.

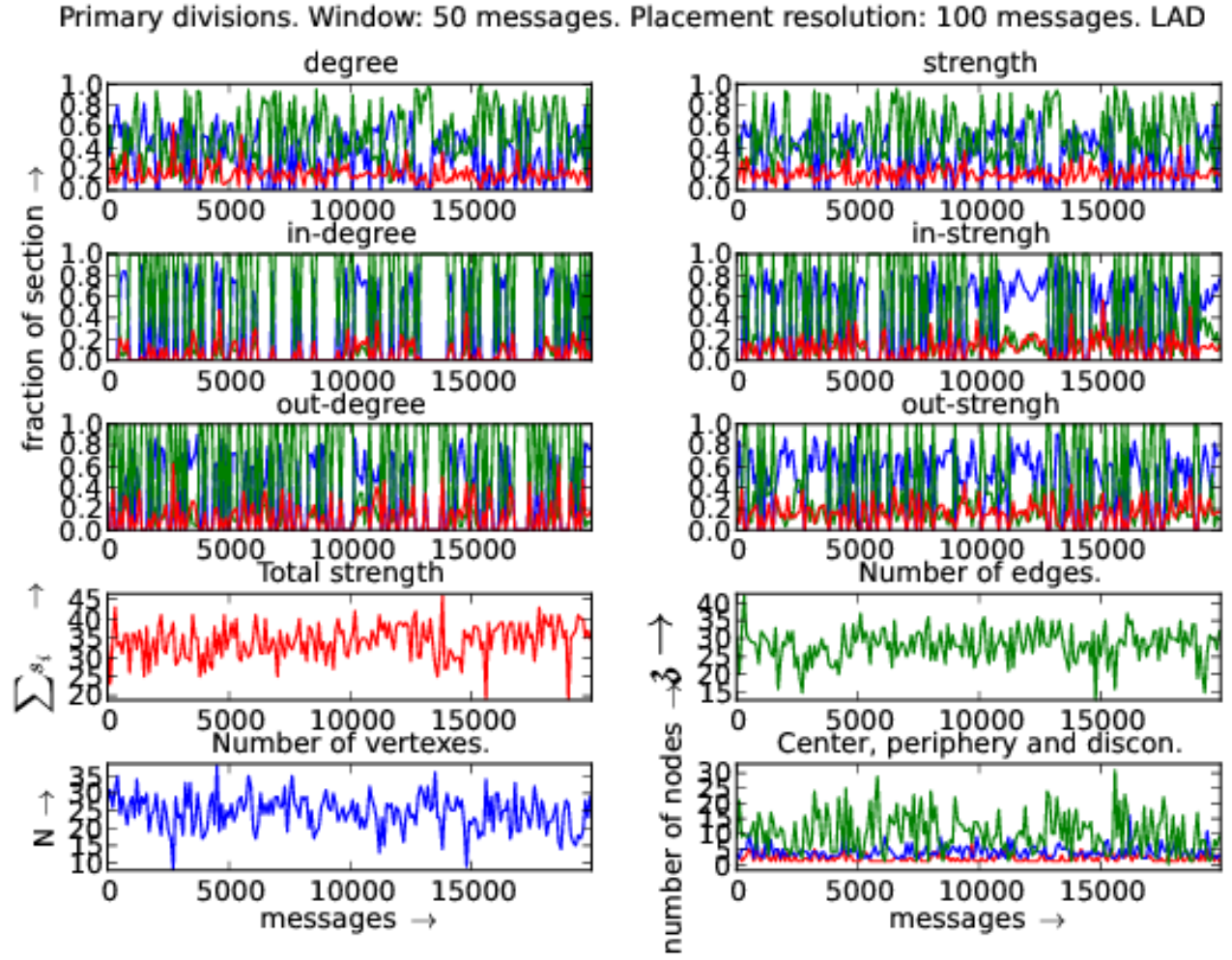


FIG. 32. Distribution of vertices with respect to each centrality measure: in and out degrees and strengths. Linux Audio Users (LAD) official mailing list. In the first six plots, red is fraction of hubs, green is the fraction of intermediary and blue is for peripheral fraction. On the last plot, red is the center (maximum distance to another vertex is equal to radius), blue is periphery (maximum distance equals to diameter) of the giant component. On the same graph, green counts the disconnected vertices.

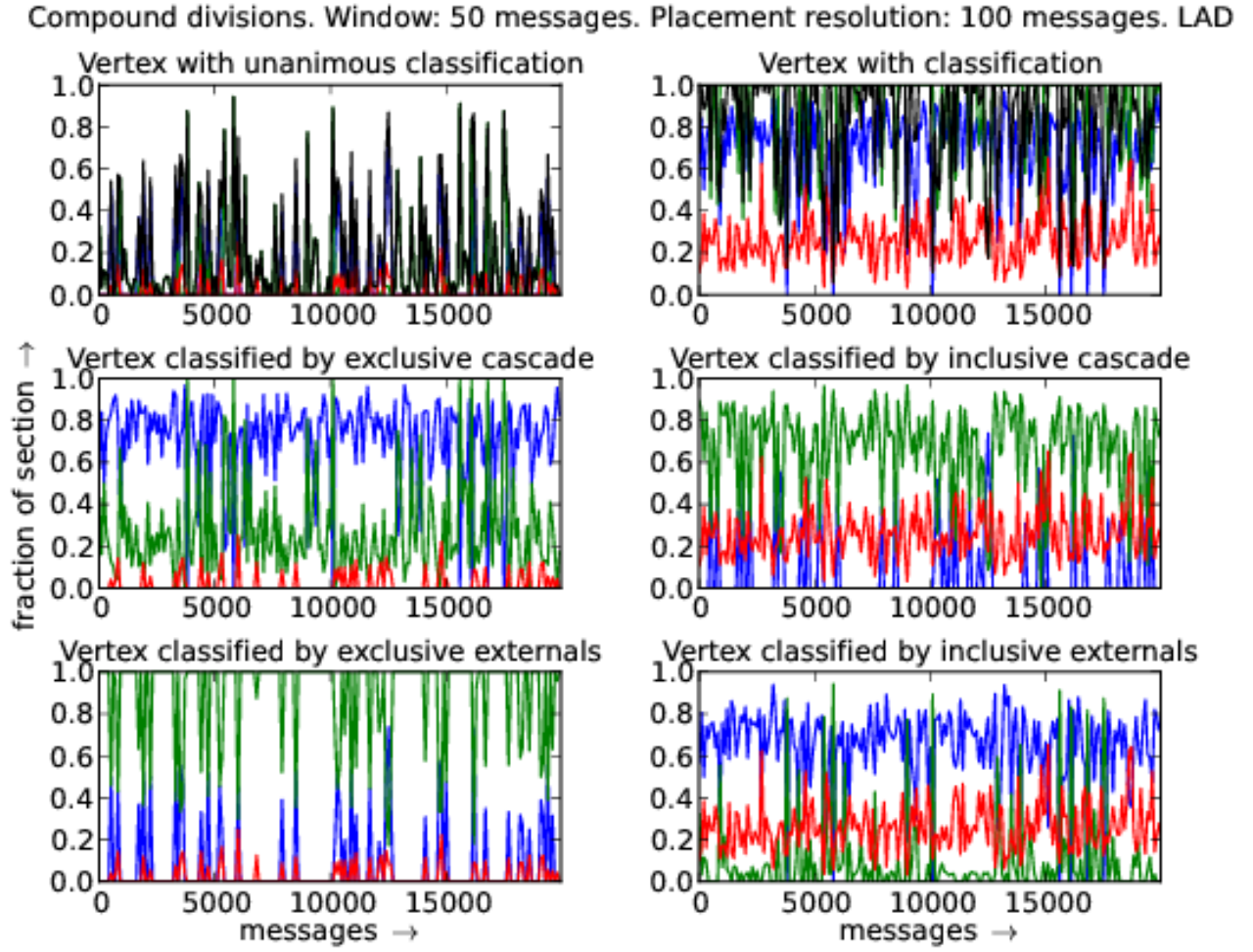


FIG. 33. Distribution of vertex with respect to compound criteria. Red, green and blue designate hubs, intermediary and border (peripheral) vertex fractions. The first two plots exhibit classifications that are not functions. Thus, in the first plot, the fraction of vertices with unique classification is plotted in black. On the second plot, black represents the fraction of vertices that has more than one class: $\frac{\text{number of classifications} - \text{number of nodes}}{\text{number of nodes}}$. Compound criteria is described in Section III B 1.